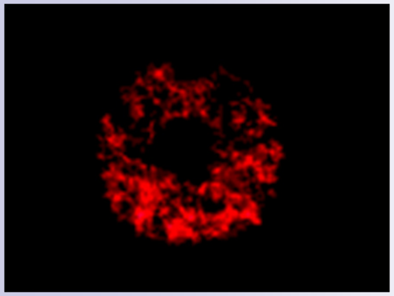

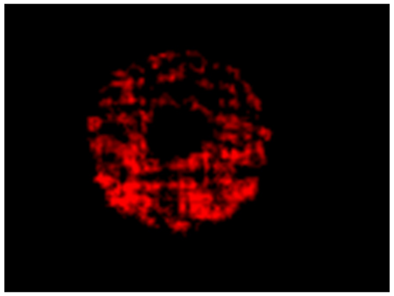

The Effects of the Atmosphere on Propagating Laser Beams, Plenoptic Sensors, and Adaptive Optics

Christopher C. Davis
Department of Electrical and Computer Engineering
University of Maryland, College Park

ECE Department Advisory Board 7-8-16

The Maryland Optics Group

Acknowledgments

- Professor Ron Phillips , UCF
- Professor Larry Andrews, UCF
- Robert Crabbs, UCF
- Dr. John Rzasa, UMD
- Dr. Chensheng Wu, UMD
- Jonathan Ko, UMD
- Dr. Billy Nelson, UMD
- Joint Technology Office (JTO)
- Office of Naval Research (ONR)

The Atmosphere Distorts Laser Beams and Imagery

- Scintillation
- Refraction
- Scattering
- High Power beams produce "Thermal Blooming"

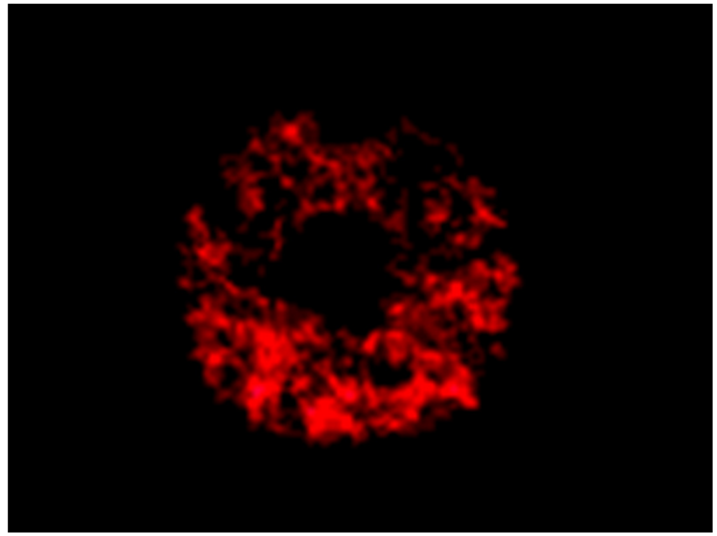

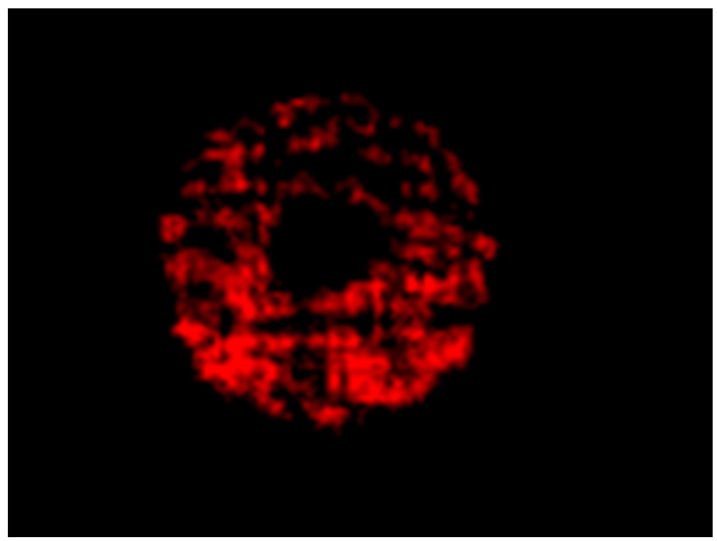

The Atmosphere is a Fluctuating Random Medium

- Obscuration
  - Aerosols
  - Rain, Snow
  - Pollution
  - 0.5 dB/km clear air, 3 dB/km haze, >50 dB/km dense fog
- Turbulence
  - Characterized by the refractive index structure constant C_n^2 $m^{-2/3}$
- Wind
- Ice crystals

Why is Laser Beam Propagation through the Atmosphere Important?

- Fundamental understanding of atmospheric effects
  - Obscuration
  - Turbulence
    - Scintillation
    - Aperture averaging
- Free Space Optics (FSO)
  - Optical communication through the atmosphere
  - Imaging through the atmosphere
- Optical sensing through the atmosphere
- Laser Weapons

Synopsis

1. Principle of the plenoptic sensor.
2. Imaging and reconstruction mechanisms.
3. Turbulence correction
4. Imaging through turbulence
5. Additional application scenarios

Structure of a Plenoptic Sensor

Note: the hardware design of the plenoptic sensor features a Keplerian telescope array with shared objective lens.

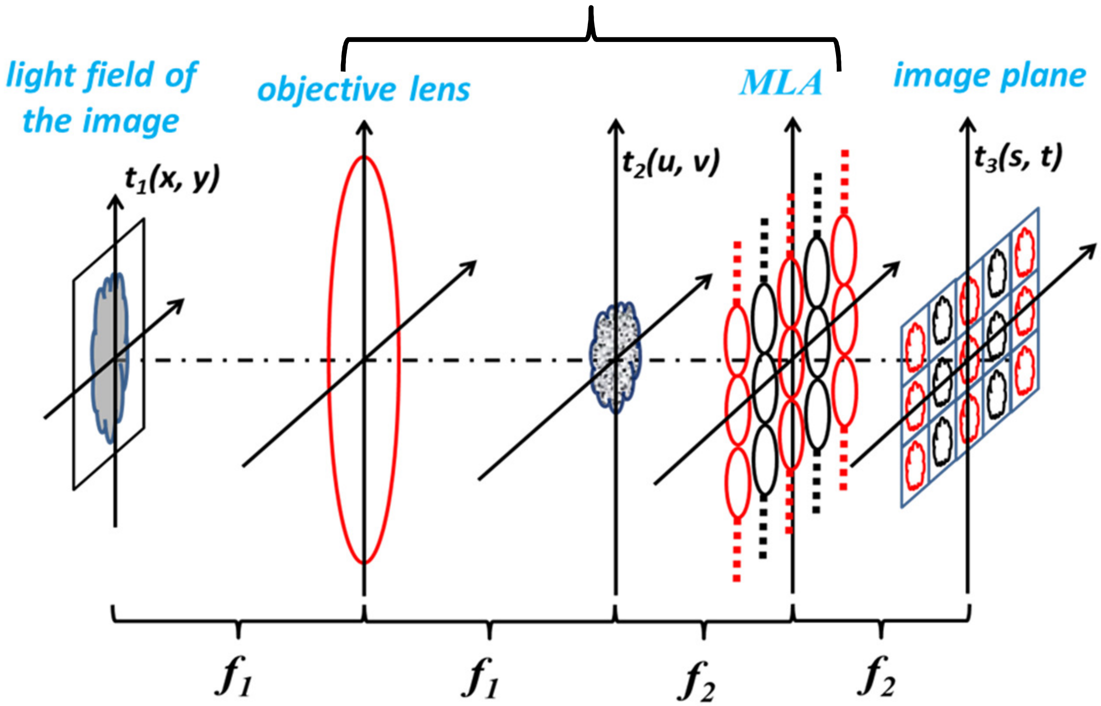

3D Structure Diagram of a Plenoptic Sensor

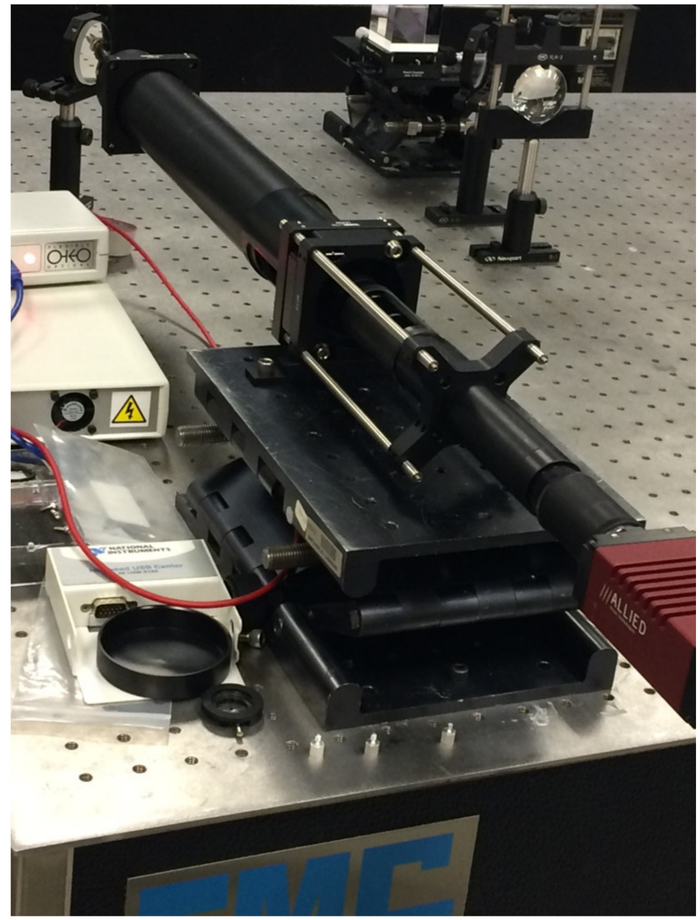

Image of a plenoptic sensor (2nd generation)

Mechanisms (wave model)

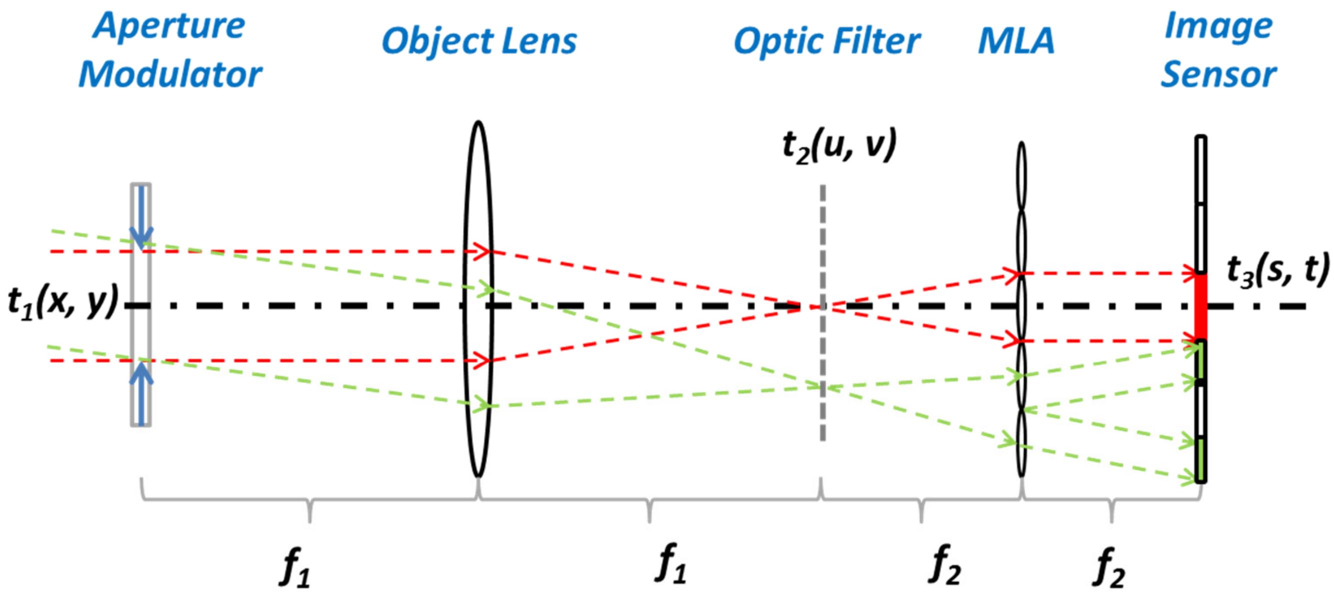

$$t_2(u,v) = \frac{1}{j\lambda f_1}\mathbb{F}\{t_1(x,y)\}\left(\frac{u}{\lambda f_1},\frac{v}{\lambda f_1}\right)$$

Spatial Fourier Transform

$$t_3(s,t) = \sum_{M,N} t_3^{M,N}(s',t')$$

$s' = s - Md; \qquad t' = t - Nd$

Each lens unit performs a second local Fourier Transform

$$t_3^{M,N}(s',t') = -\frac{1}{\lambda^2 f_1 f_2}\iint \mathbb{F}\{t_1(x,y)\}\left(\frac{u'+Md}{\lambda f_1},\frac{v'+Nd}{\lambda f_1}\right) rect\left(\frac{u'+s'}{d}\right) rect\left(\frac{v'+t'}{d}\right) e^{-j\frac{2\pi}{\lambda f_2}(u's'+v't')} du'dv'$$

$u' = u - Md; \qquad v' = v - Nd$

Transform kernels that produce a scaled reverse image

Basic Experimental Platform for Testing the Principles of a Plenoptic Sensor

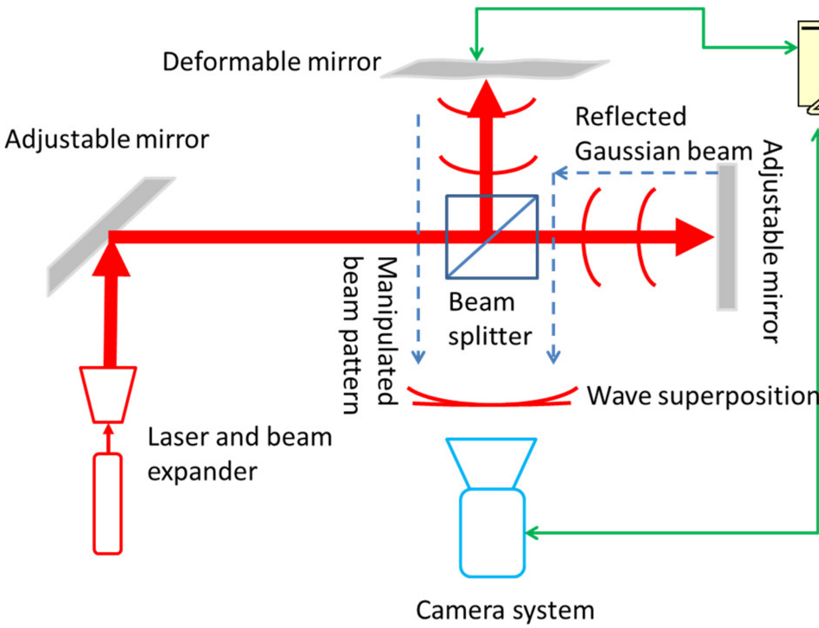

Detecting wavefront distortion with interferometer/plenoptic sensor

Picture of experiment layout

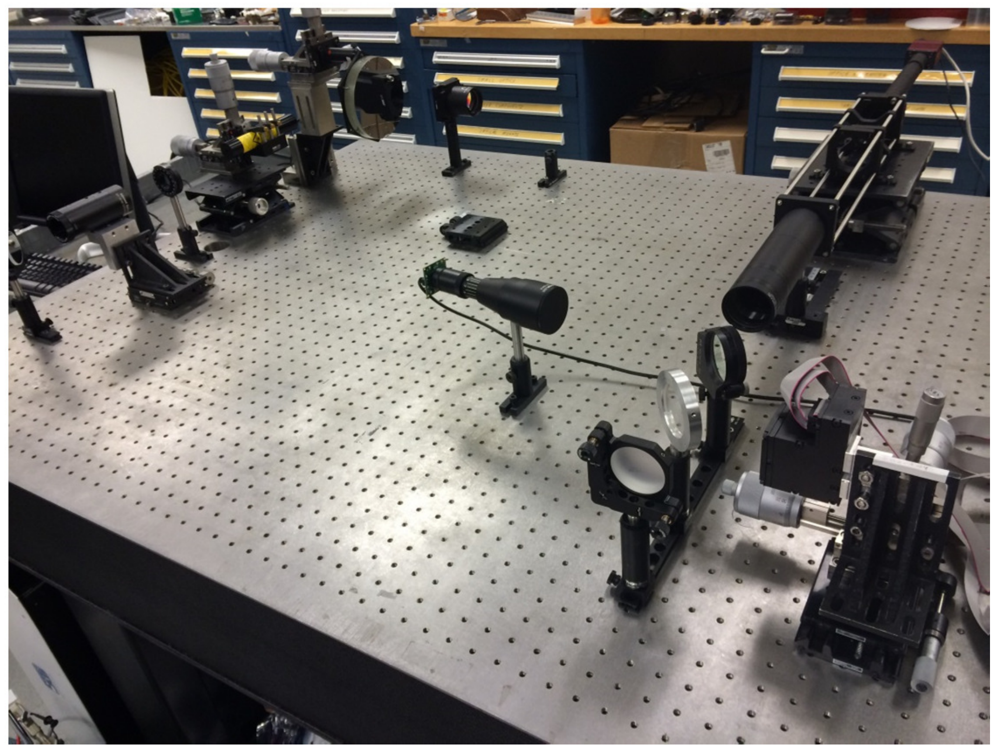

Illustrative Example of Wave Analysis on the Plenoptic Sensor

The plenoptic image of a Gaussian beam with "Trefoil" phase deformation:

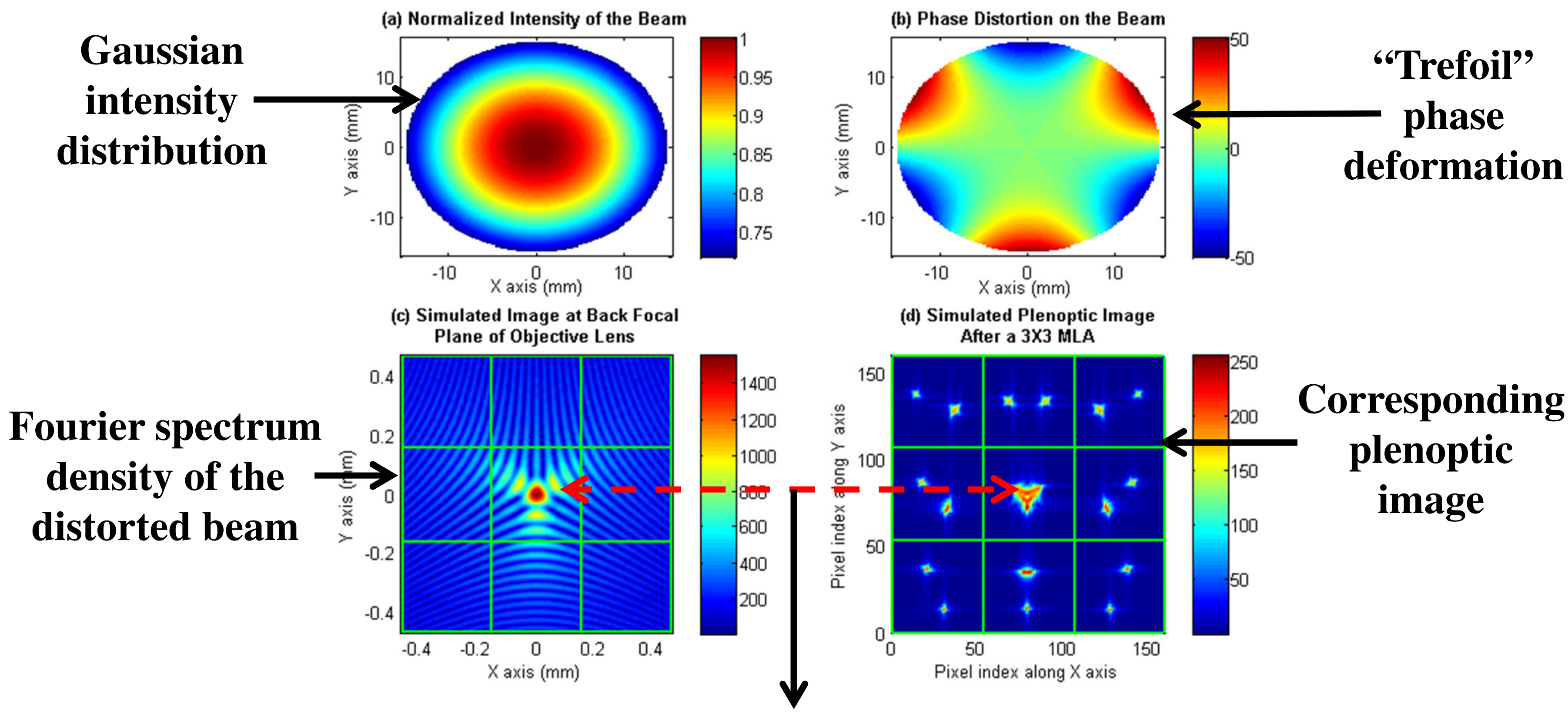

Each cell samples and solves one or more sub-Fourier spectra

An Image Example

A "Trefoil" phase distorted Gaussian Beam (Zernike Z_3^3):

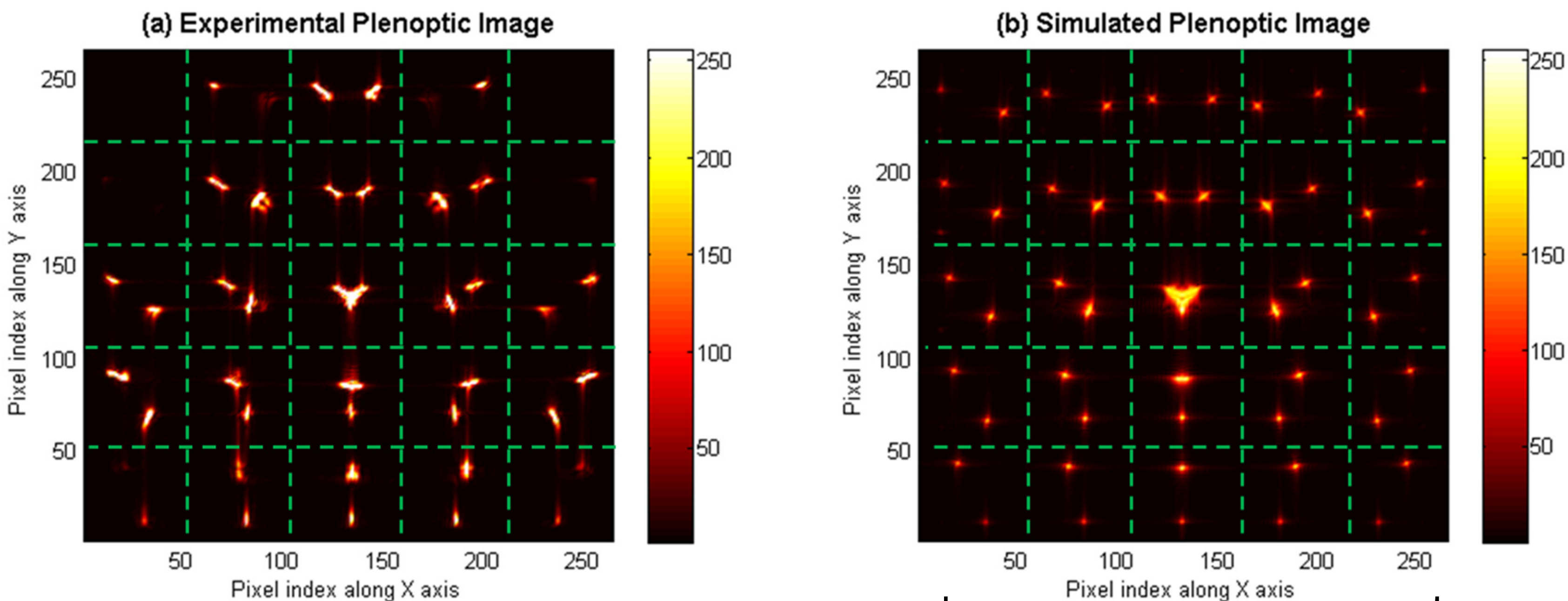

Fourier Spectrum of a Coherent Beam: $(f_x, f_y) \Leftrightarrow (m,n)$ ⇨ **Spectrum can be retrieved by cell indices**

$$U(x,y) = \sum_i U_i(x,y) = \sum_i A_i(x,y) \exp\left[j\left(f_x \cdot x + f_y \cdot y \right) + j\varphi_i \right]$$

⇨ **Amplitude can be retrieved by intensity distribution in a cell**

Experimental Reconstruction Result of the "Trefoil" Phase

Phase distortion ***Fourier Spectrum***

Experiment:

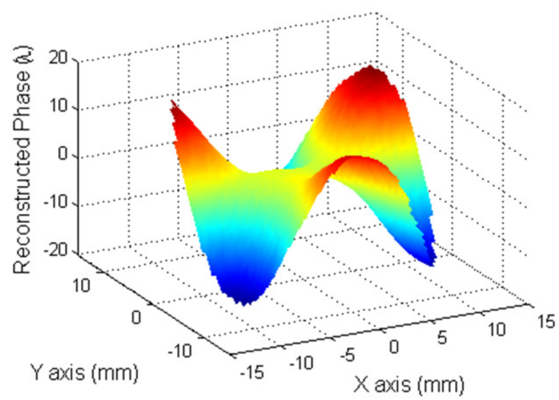

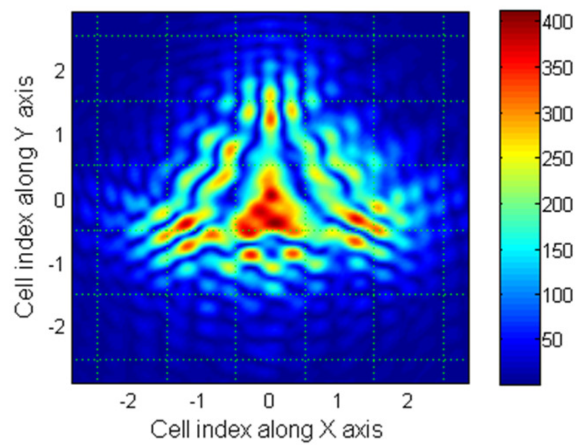

Actual distortion:

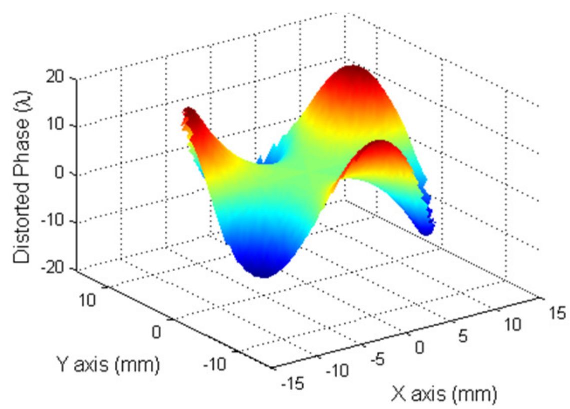

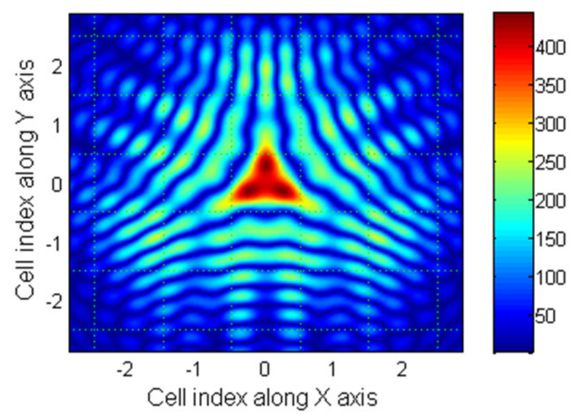

Additional Examples

Plenoptic image ***Phase distortion*** ***Fourier spectrum***

Coma:

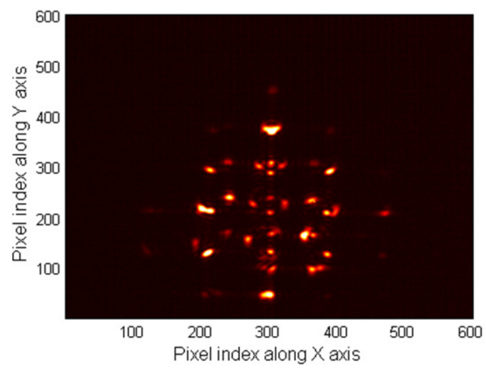

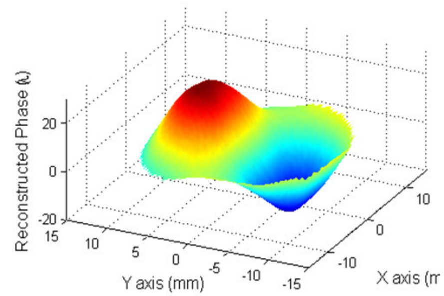

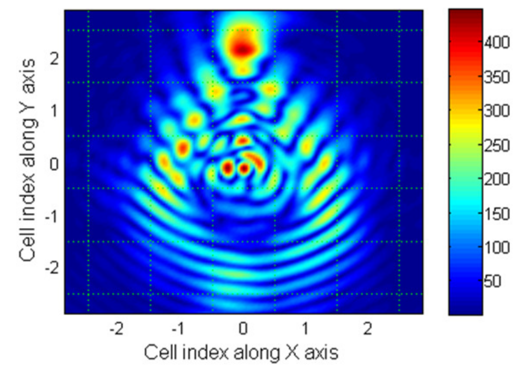

Astigmatism:

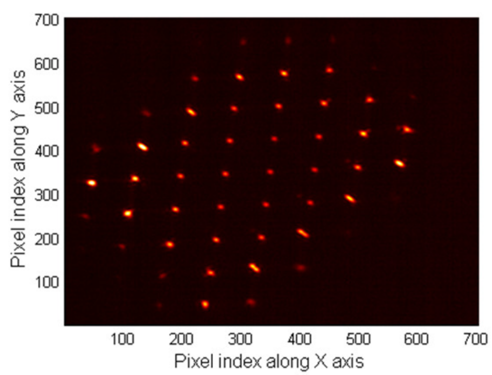

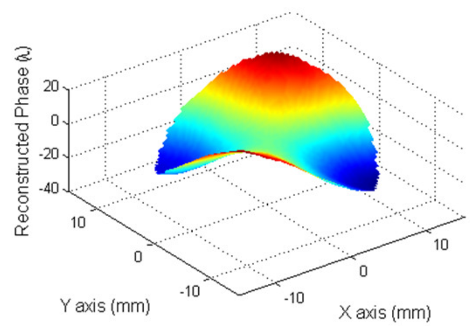

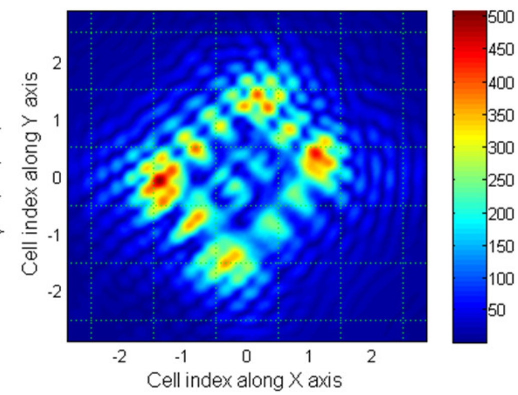

Additional Examples

Plenoptic image ***Phase distortion*** ***Fourier spectrum***

Defocus:

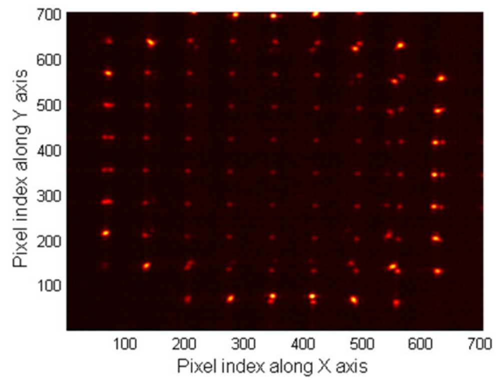

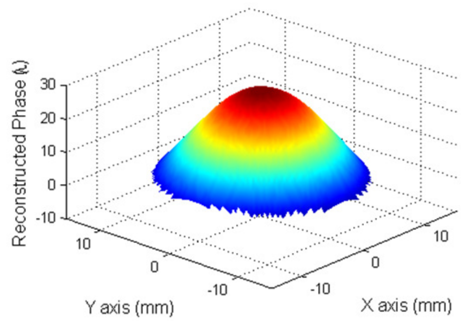

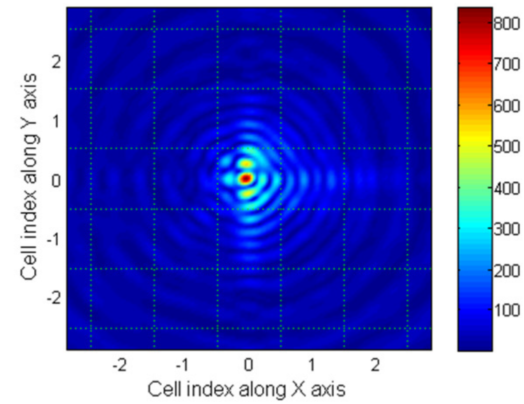

Diamond:

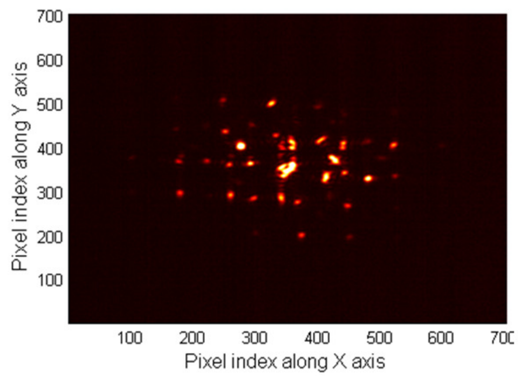

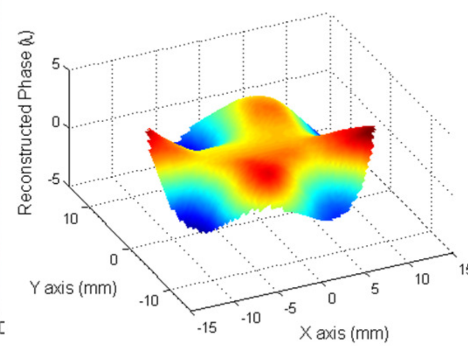

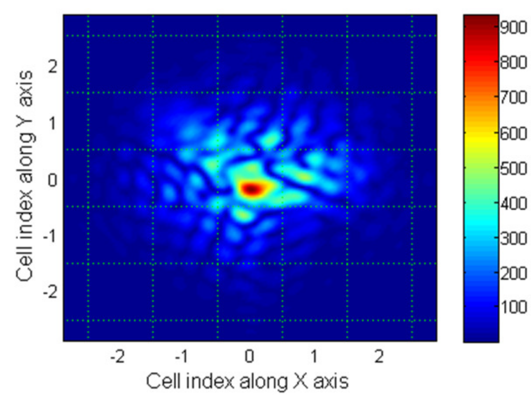

Fundamental Results for Phase Reconstruction

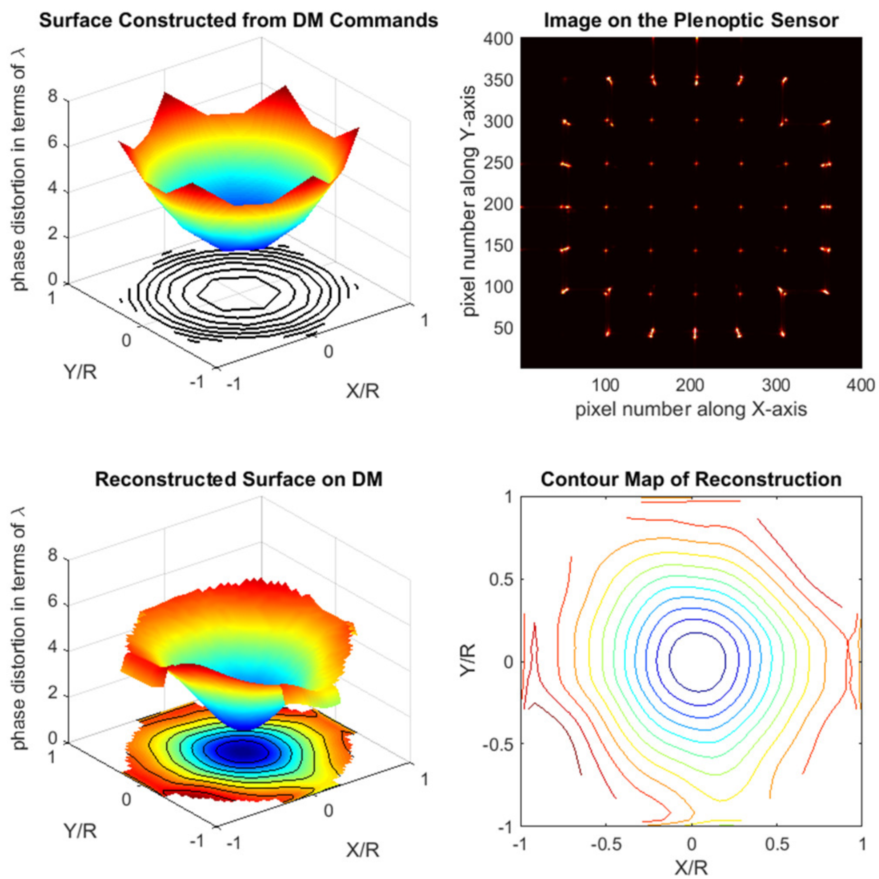

Zernike(M=2,N=0) on the plenoptic sensor

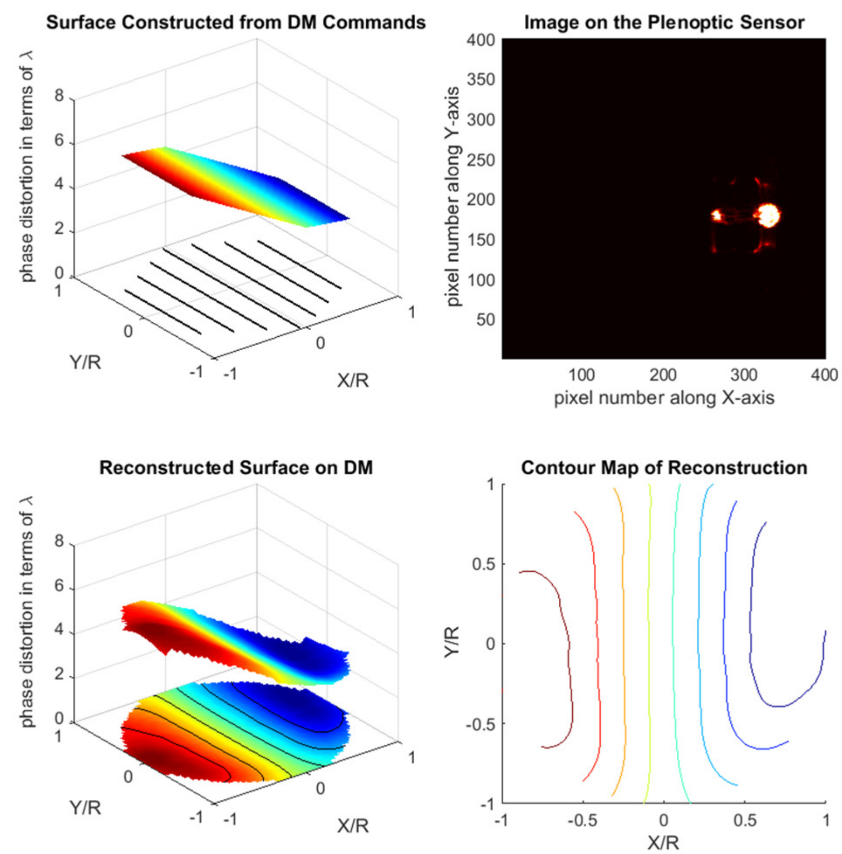

Zernike(M=1,N=1) on the plenoptic sensor

Fundamental Results for Phase Reconstruction

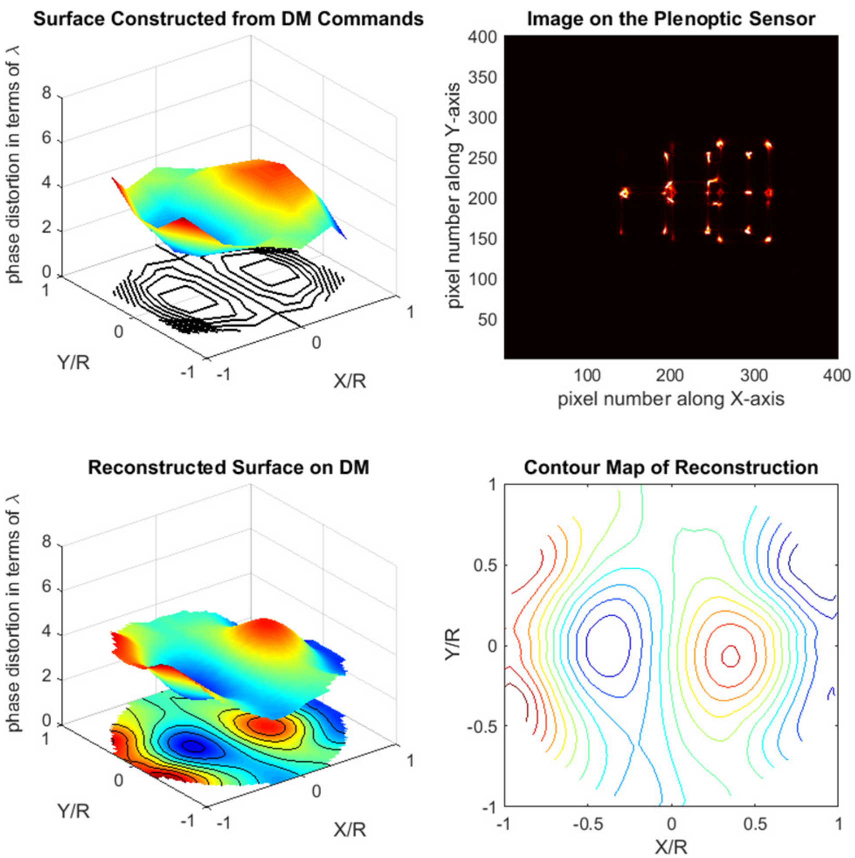

Zernike(M=3,N=1) on
the plenoptic sensor

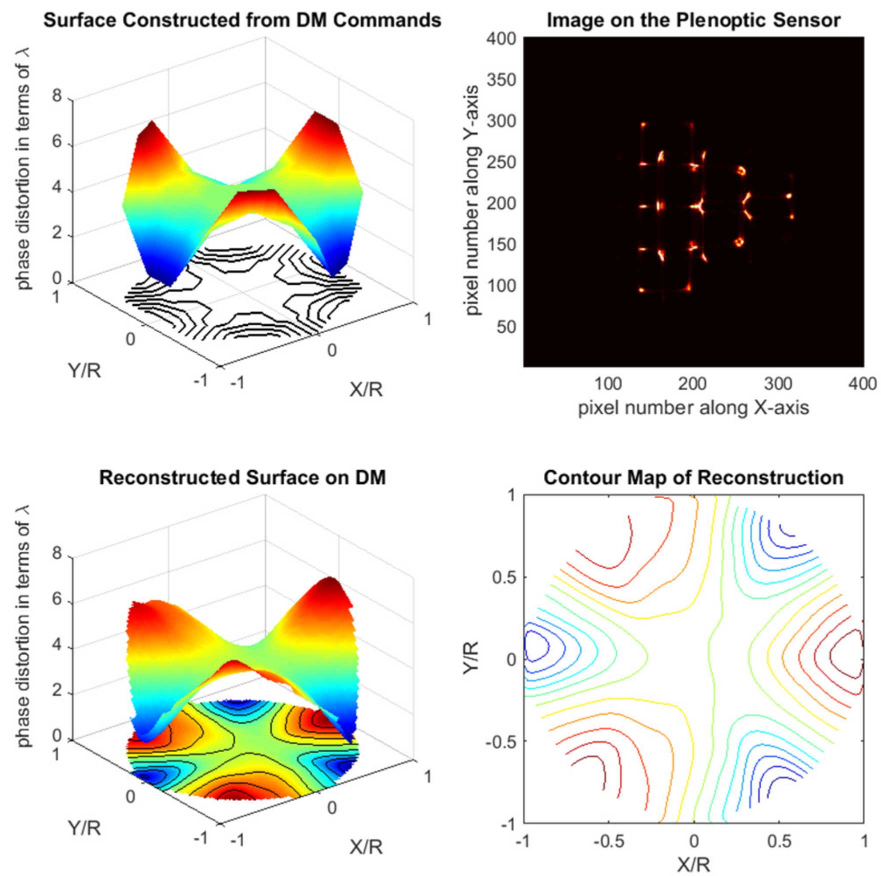

Zernike(M=3,N=3) on
the plenoptic sensor

Fundamental Results for Phase Reconstruction

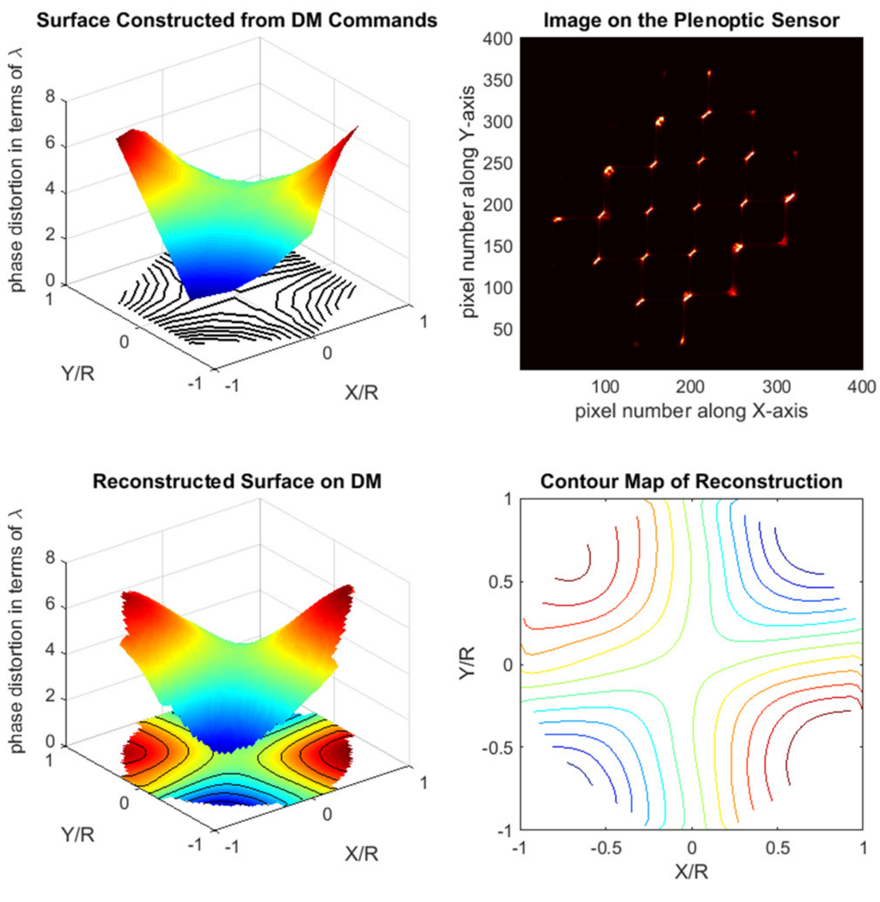

Zernike(M=2,N=2) on the plenoptic sensor

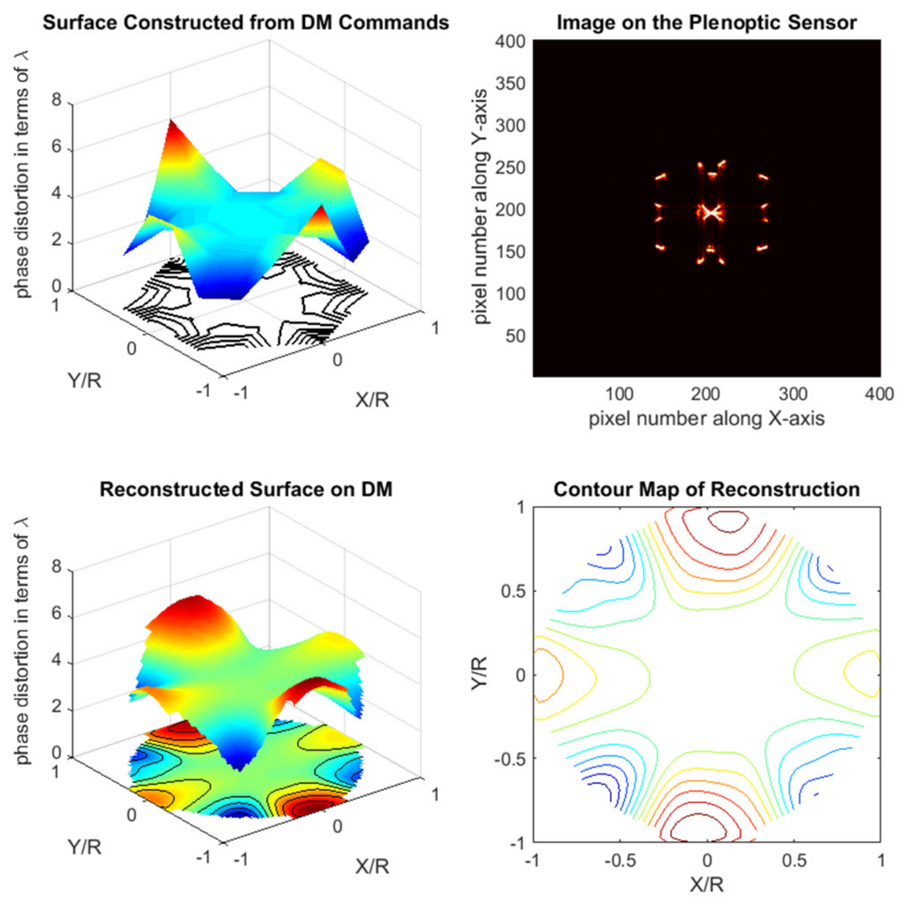

Zernike(M=4,N=4) on the plenoptic sensor

Fast Reconstruction Algorithm

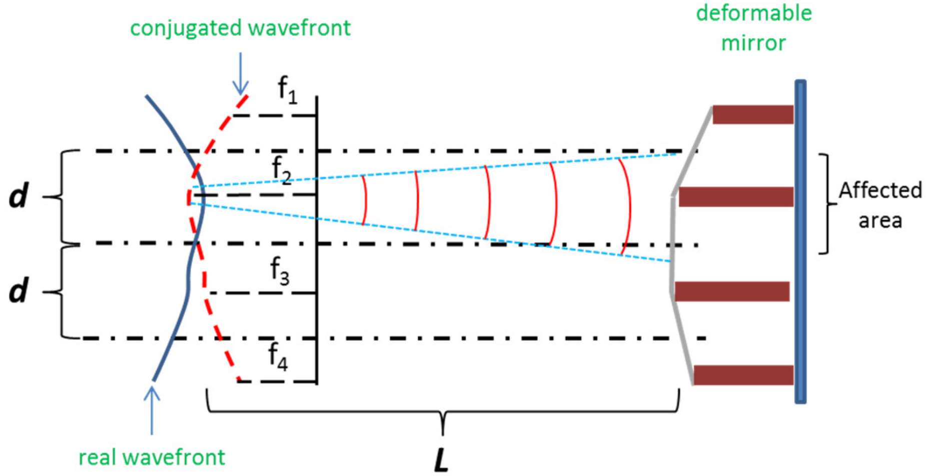

Build vertices based on AO device

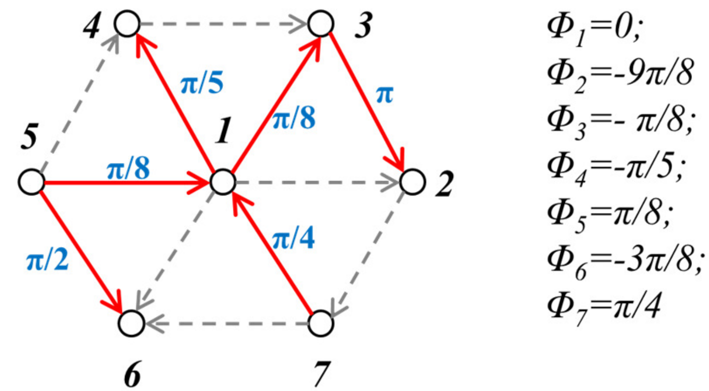

Require only one "tree" to solve

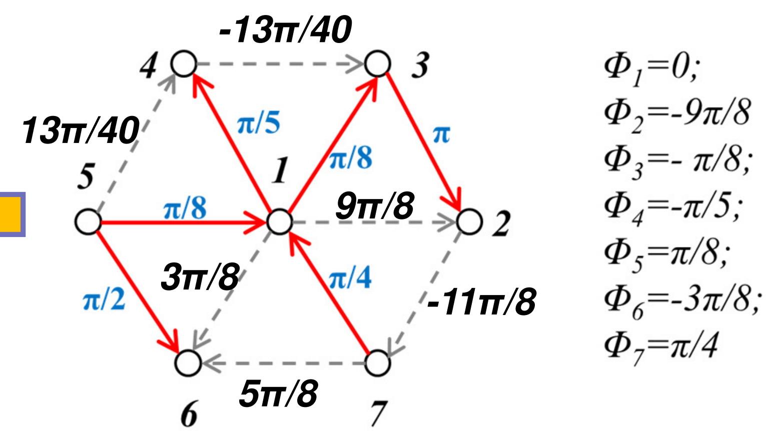

The remaining information of the digraph can be easily solved

Problem: how these edges are selected?

1) In general, more intensity means more "informative".
2) Only counts the pixels on the edges.
3) Each edge (contains 9 pixels) forms a exclusive "counting" box.
4) If the DM is a 37 channel, only 36 edges are required to form a fast reconstruction.

Fast reconstruction (graph theory)

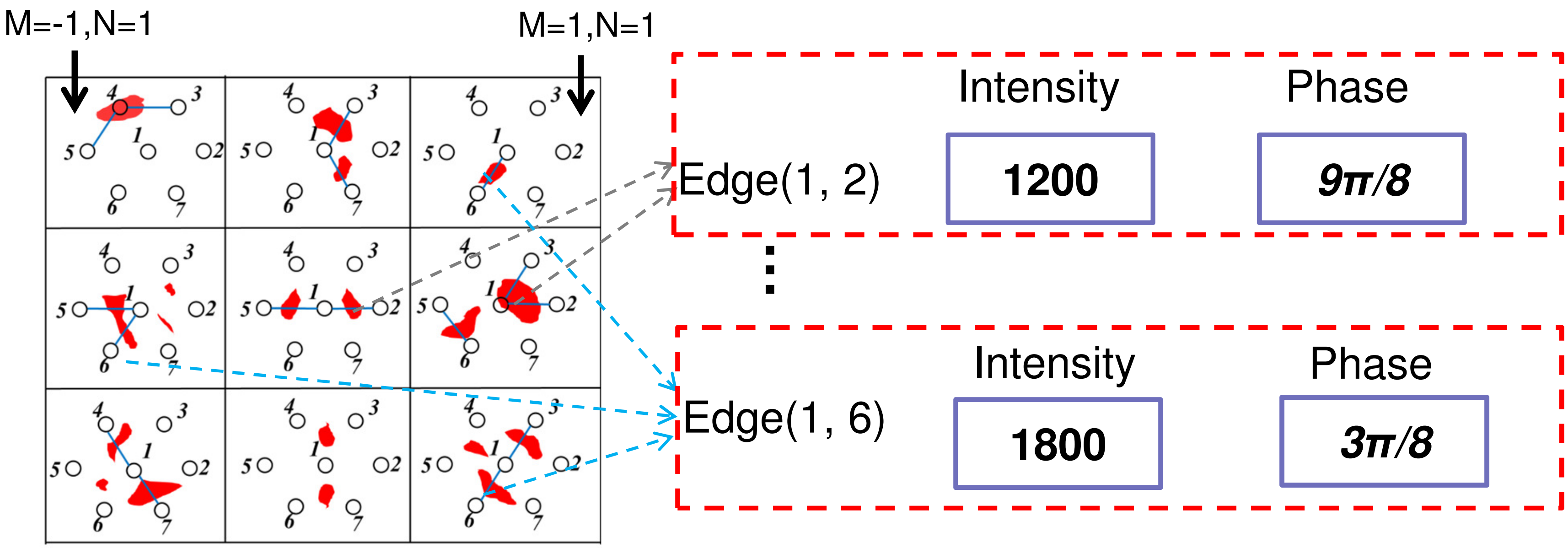

Assumptions:

1) "Red" area a highly illuminated pixels (namely >100 in value).
2) Geometric copies of the vertices are shown on the plenoptic image.
3) Once an illuminated patch falls on the edge, its intensity is counted.
4) Each pixel in "red" represents phase change of (MΔφ, NΔφ).

Edge selection rules:

1) Edge(1, 6) has higher intensity sums than edge (1, 2). Thus it should be considered before edge (1, 2).
2) Edges are sorted in descend order by the overall intensity.
3) If the current branch doesn't form a circuit, add it to the tree structure.

Fast reconstruction (graph theory)

Assume the sorted edges are:

1. Edge(1, 3)
2. Edge(1, 4)
3. Edge(2, 3)
4. Edge(1, 5)
5. Edge(5, 6)
6. Edge(4, 5)
7. Edge(1, 6)
8. Edge(1, 2)
9. Edge(1, 7)
10. Edge(3, 4)
11. Edge(2, 7)
12. Edge(6, 7)

Descend in intensity

{1}, {2}, {3}, {4}, {5}, {6}, {7}

Step 1: combine 1, 3

{1,3}, {2}, {4}, {5}, {6}, {7}

Step 2: combine 1, 4

{1,3,4}, {2}, {5}, {6}, {7}

Step 3: combine 2, 3

{1,2,3,4}, {5}, {6}, {7}

Step 4: combine 1, 5

{1,2,3,4,5}, {6}, {7}

Step 5: combine 5, 6

{1,2,3,4,5,6}, {7}

Step 6: combine 4, 5 — **Already connected** → **Discard**

Step 7: combine 1, 6 — **Already connected** → **Discard**

Step 8: combine 1, 2 — **Already connected** → **Discard**

Step 9: combine 1, 7

{1,2,3,4,5,6,7} **Tree found!**

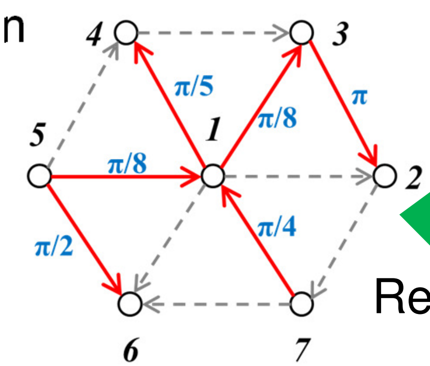

Return: tree structure

Fast reconstruction (Branch Points)

Assume for the discarded edges:

Edge(4, 5) → phase change: ***π/3***
Edge(1, 6) → phase change: ***π/2***
Edge(1, 2) → phase change: ***0***

Previously retrieved phases:

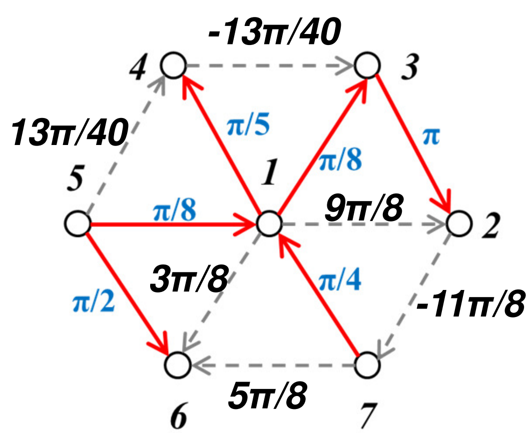

$\Phi_1=0;$
$\Phi_2=-9\pi/8$
$\Phi_3=-\pi/8;$
$\Phi_4=-\pi/5;$
$\Phi_5=\pi/8;$
$\Phi_6=-3\pi/8;$
$\Phi_7=\pi/4$

Net phase change in a loop:

Loop 1→4→5→1 : ***+π/40*** ***(small error)***
Loop 1→6→5→1 : ***-π/8*** ***(small error)***
Loop 1→2→3→1 : ***+9π/8*** ***(large disagreement)***

$$\nabla \times \nabla \varphi \neq 0$$

!! Unfortunately, a branch point happens to locate on one of the three edges: (1,2), (2,3) and (3,1).

Conclusion:

1. **Most of the branch points are avoided by the fast reconstruction algorithm.**
2. **A branch point that locates on a selected edge of the spanning tree can't be avoided (less likely to happen: P < #edge pixels/#total pixels).**

Fast Reconstruction Algorithm Fits for Dynamic Reconstruction & Correction

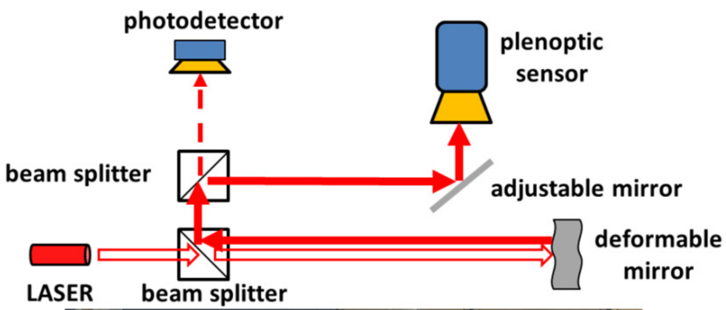

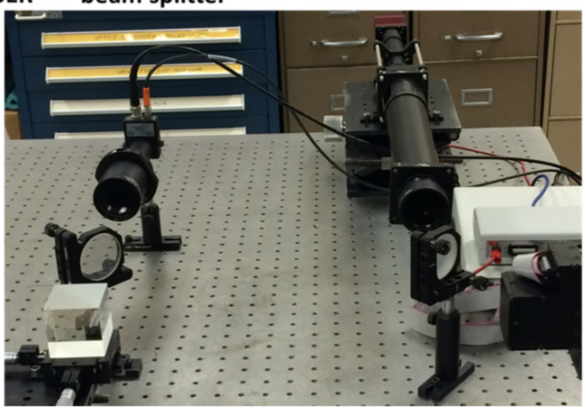

Correction results for a peak-peak phase distortion of 5.5λ in a 4m channel

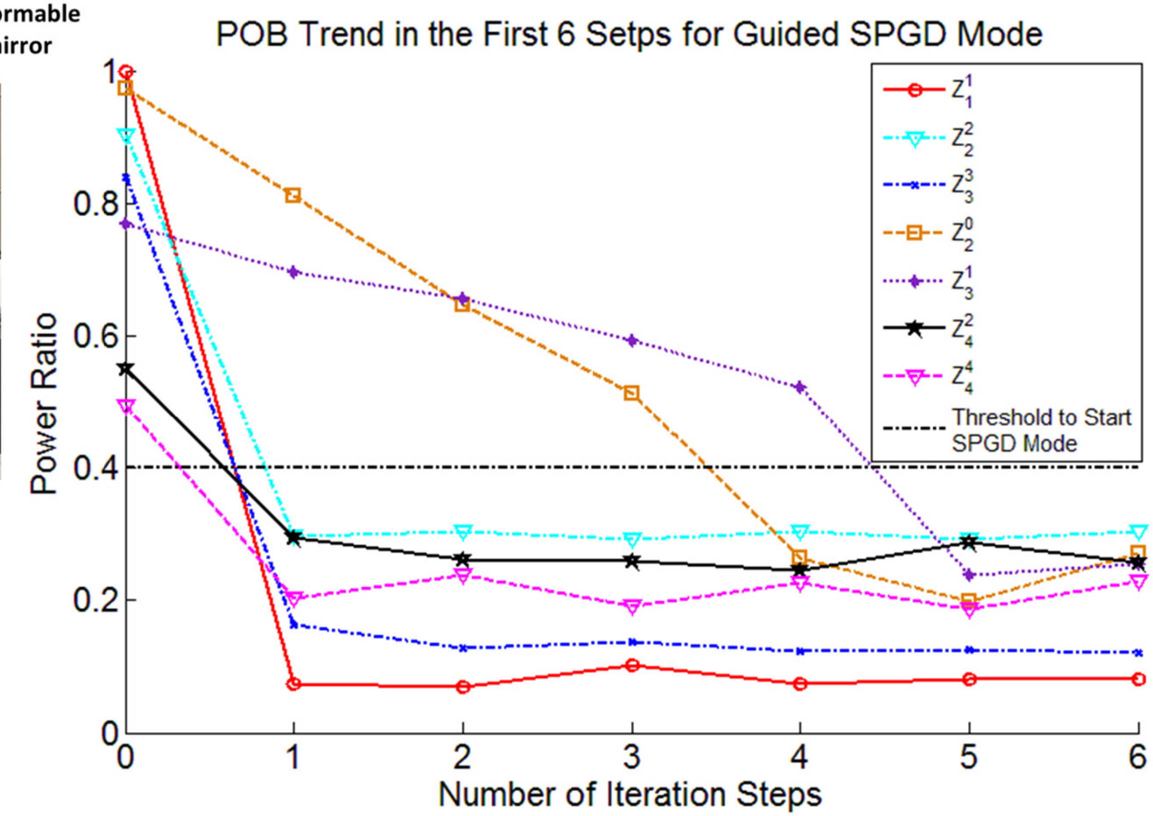

Fast reconstruction:

1. Graph theory
2. “Lossy” sensing
3. Iterative correction
4. Quick convergence

Guidance for AO systems

Comparisons with conventional SPGD:

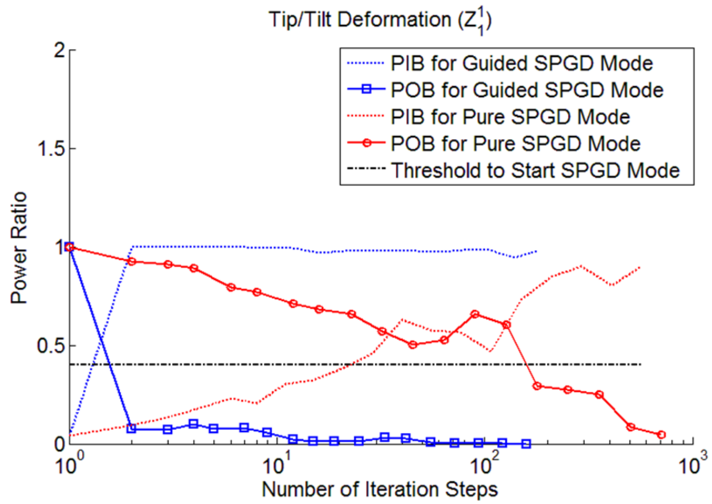

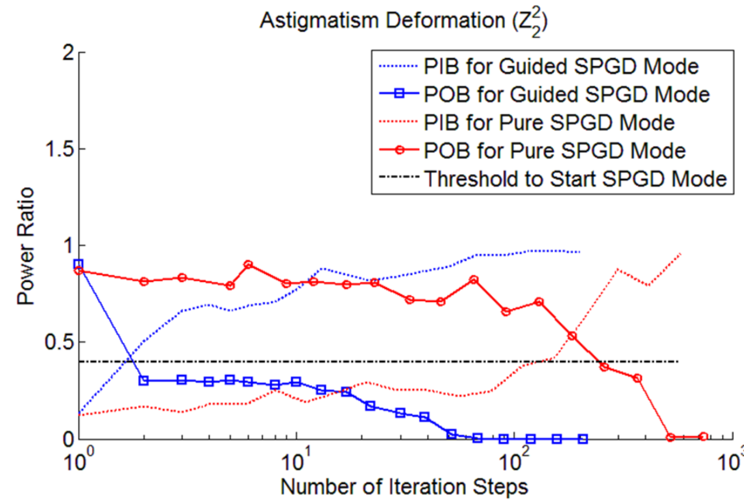

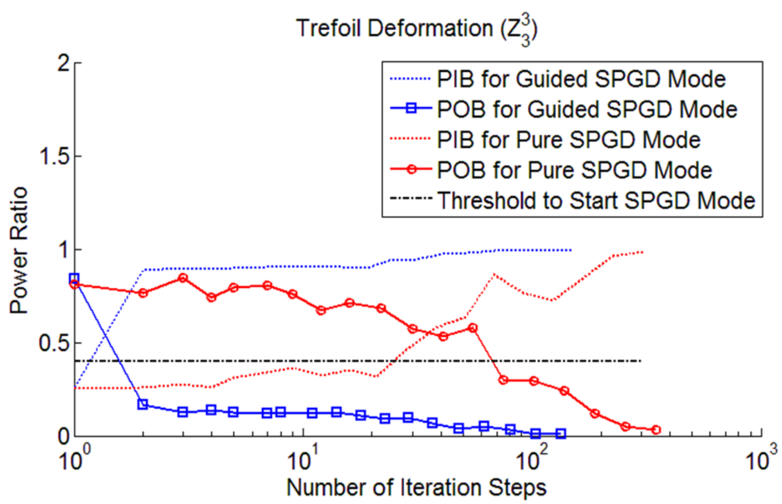

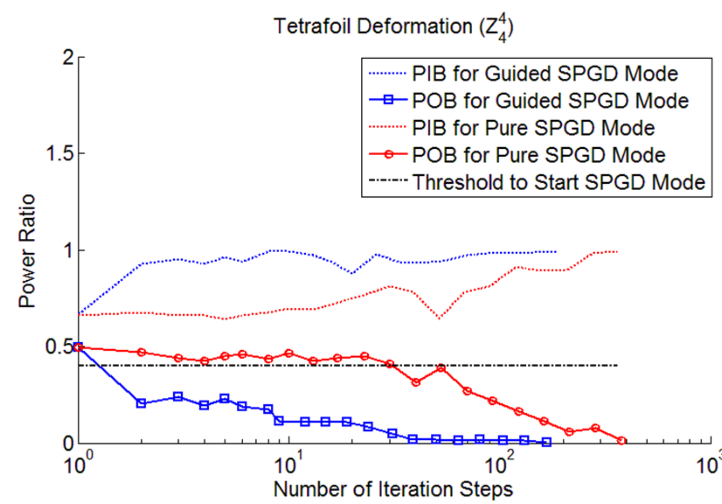

Intermediate Steps for Detecting and Correcting Large "Defocus" Phase Deformation

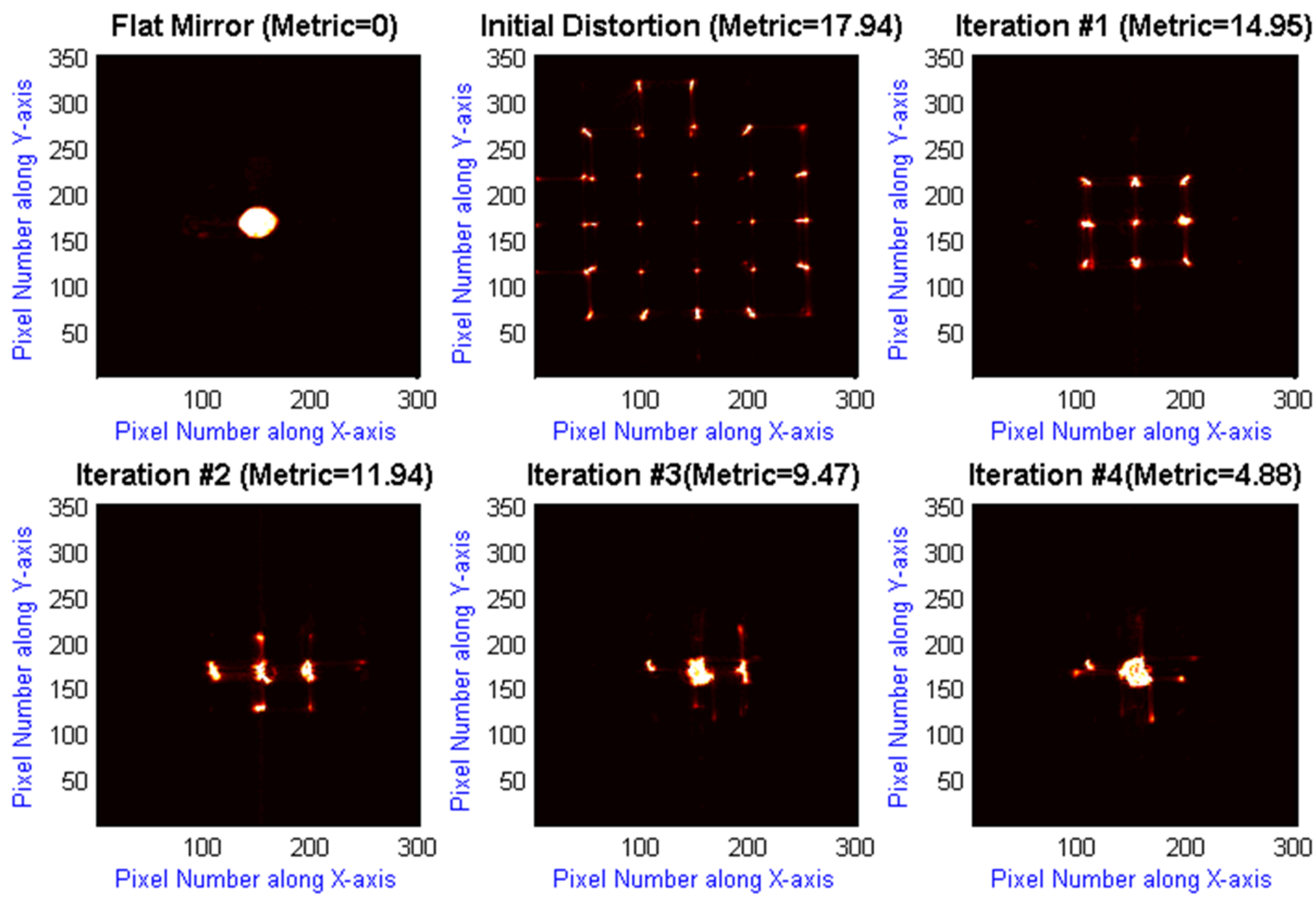

Note: A good staring point for initiating SPGD is obtained at the end of 4th step. Normal SPGD would take 600 steps to find a similar starting point.

Real Time Correction

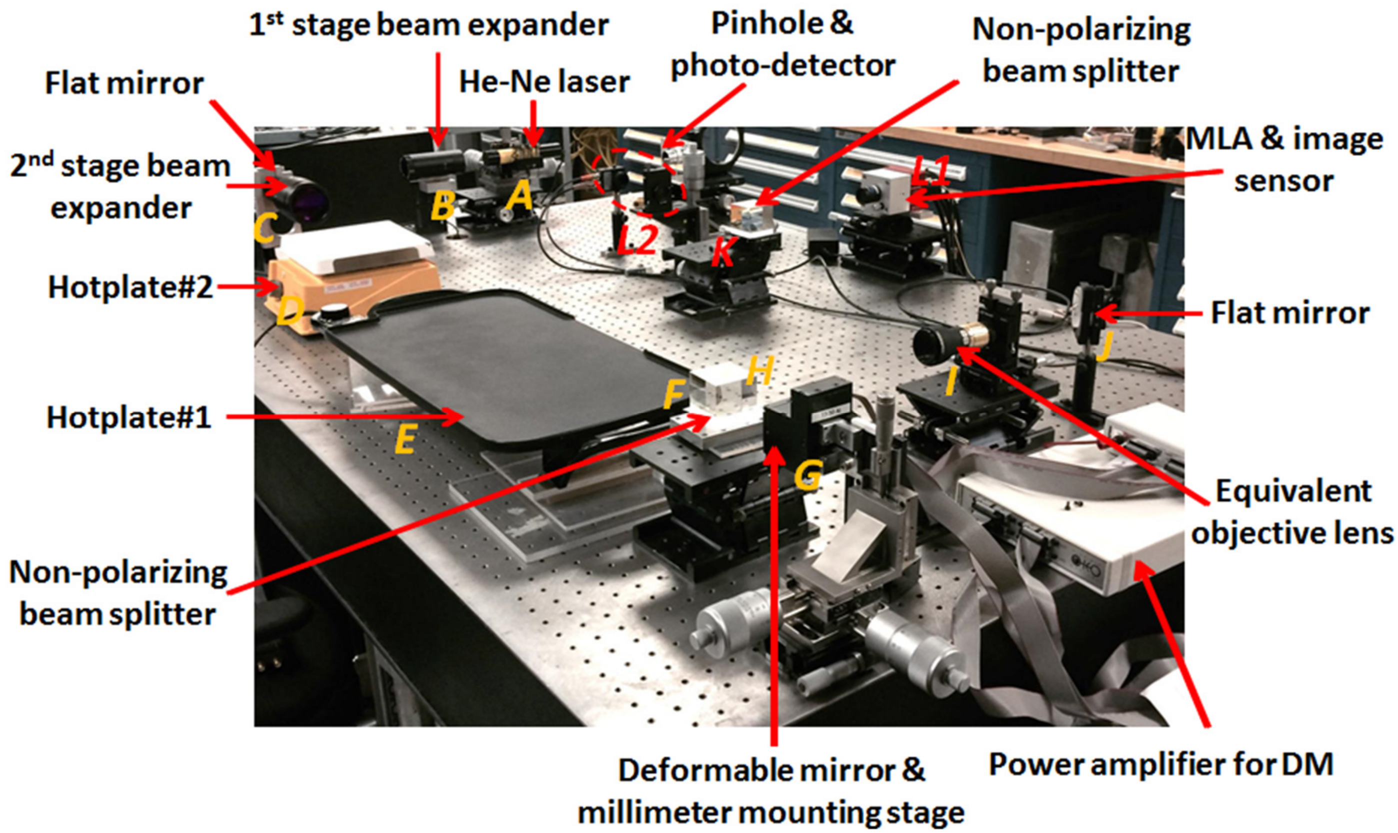

Notes:

- The laser beam propagates alphabetically
- K→L1: Plenoptic sensor that detects the wavefront distortion.
- K→L2: Photo detector that indicates how much power is focused to a tight spot.

Real Time Correction Result

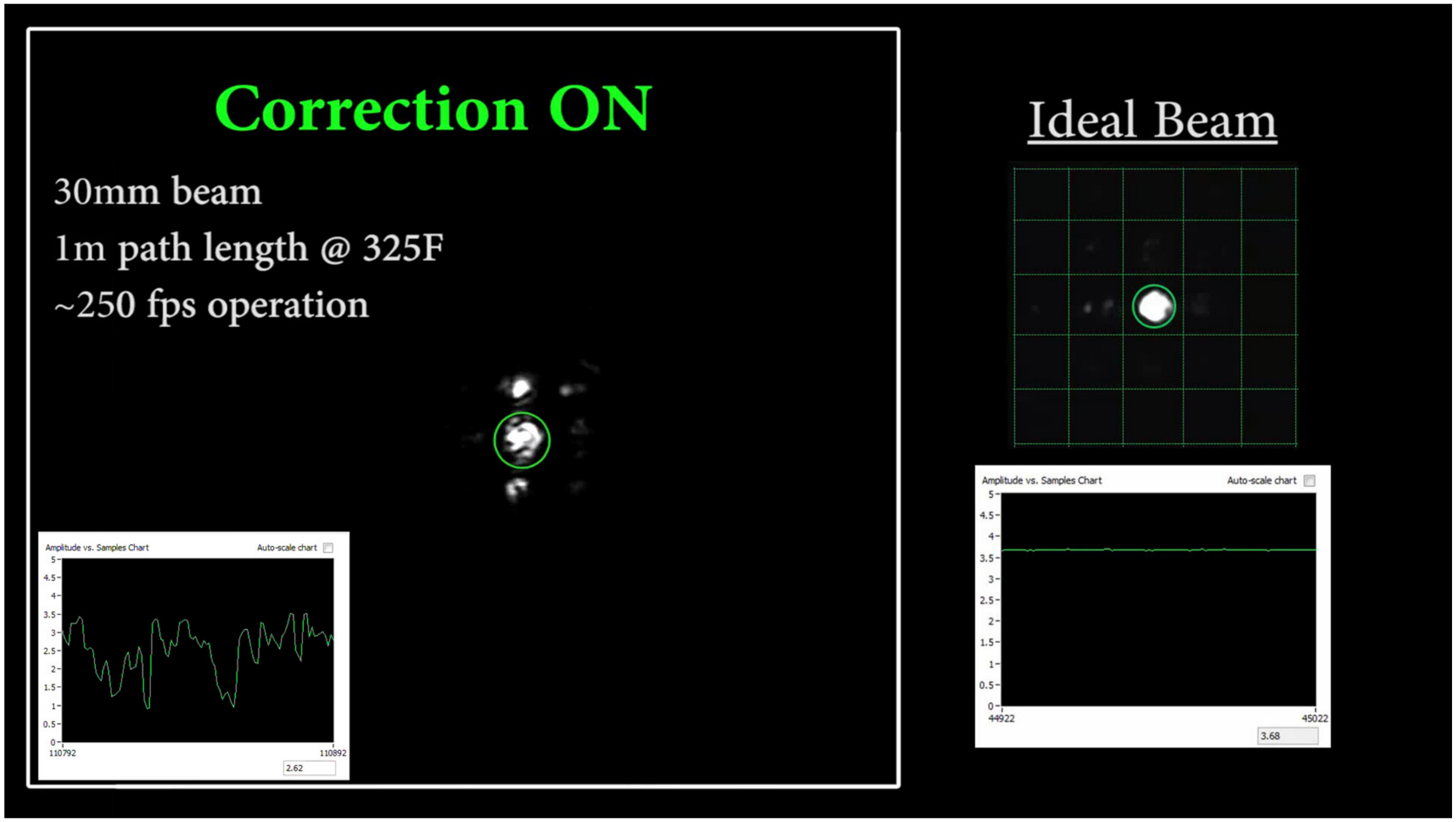

Signal Quality Analysis

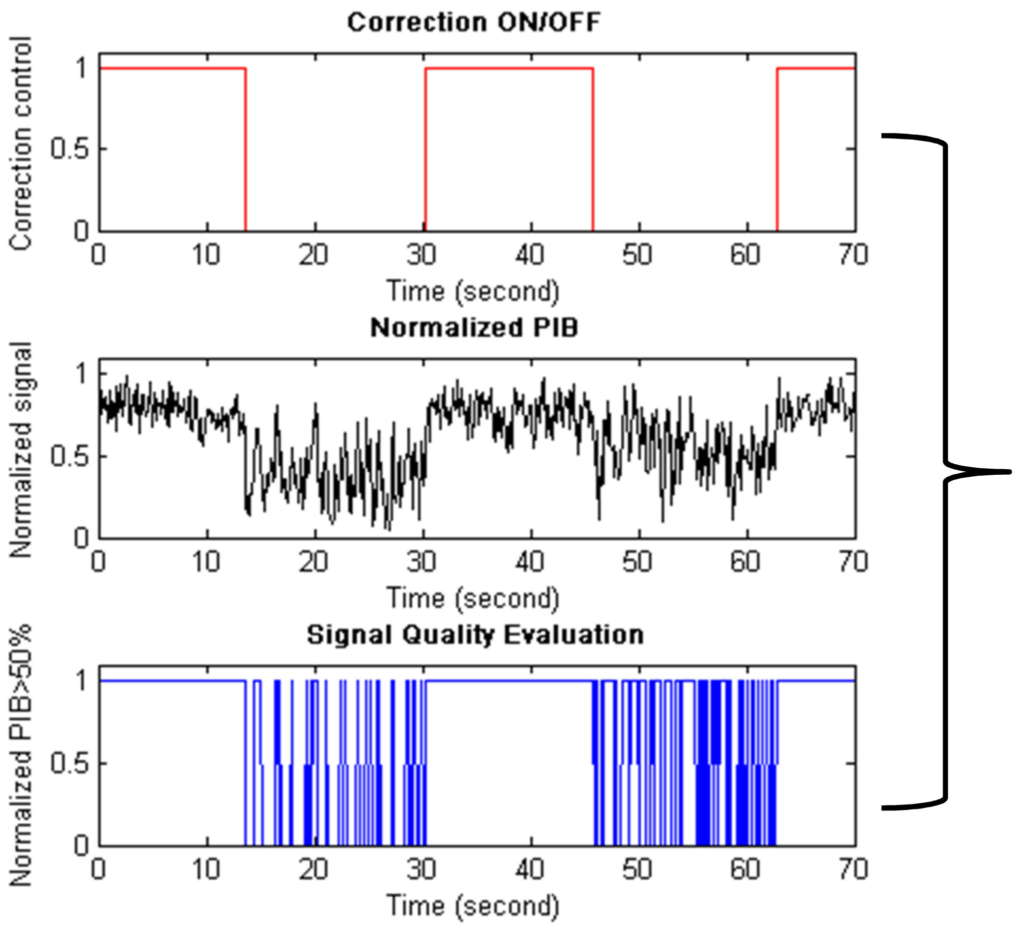

A reliable optics link is maintained during the correction circles

Comparison: Shack-Hartmann WFS Image for the Same Turbulence Condition

A normal frame example under the same turbulence condition

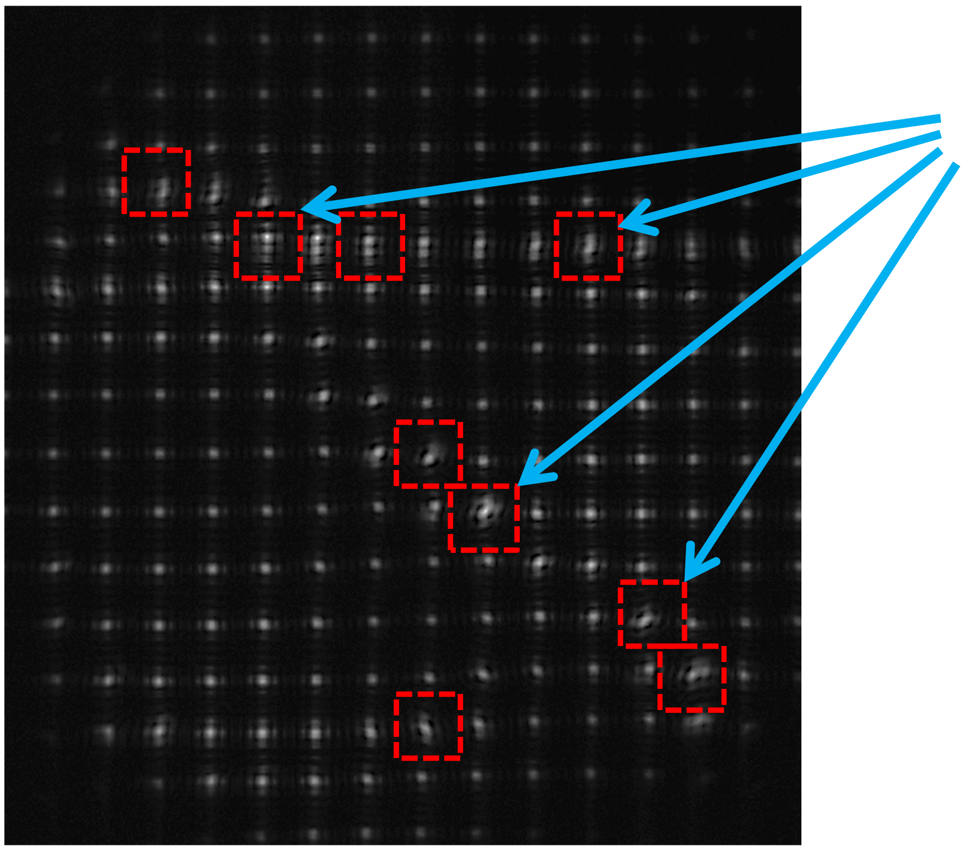

1. Overlapping patches will generate image cells of unconventional patterns, which is difficult to interpret with accurate wavefront information.
2. Each cell provides no more than 1 phase sample (when a sharp focus can be observed), the overall number of phase samples are low (around 100 samples).
3. SH reconstruction will normally fail for strong turbulence distortions.

Additional Results under 325°F turbulent channel

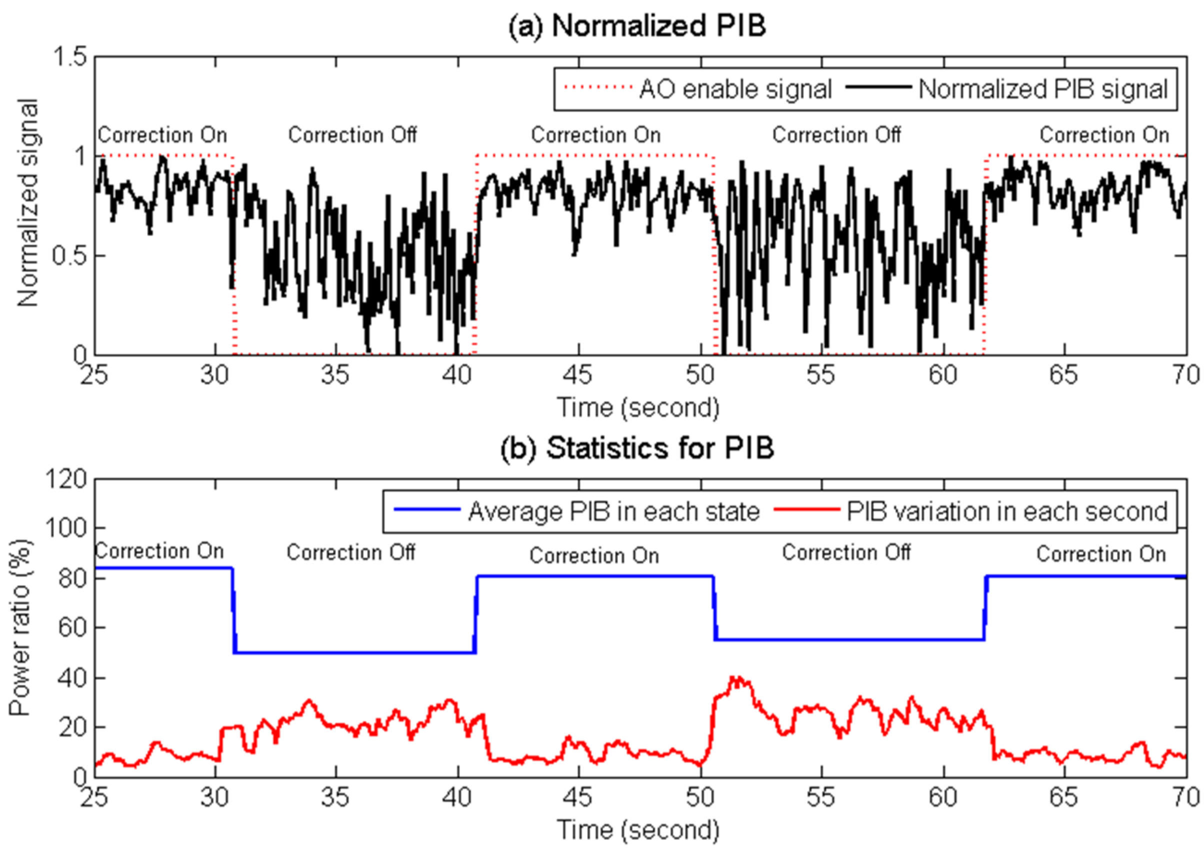

Turbulence Distorts Images

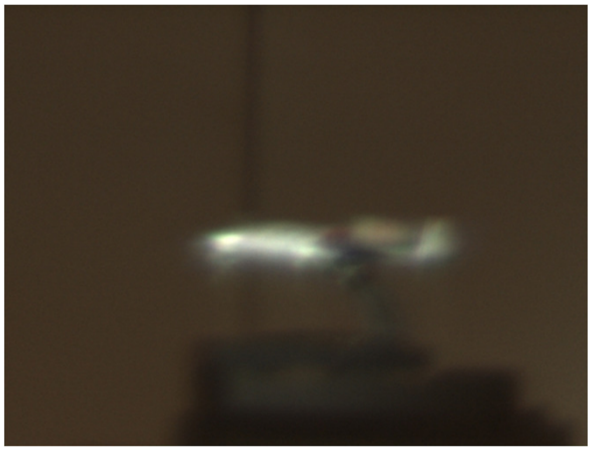

Turbulence near camera

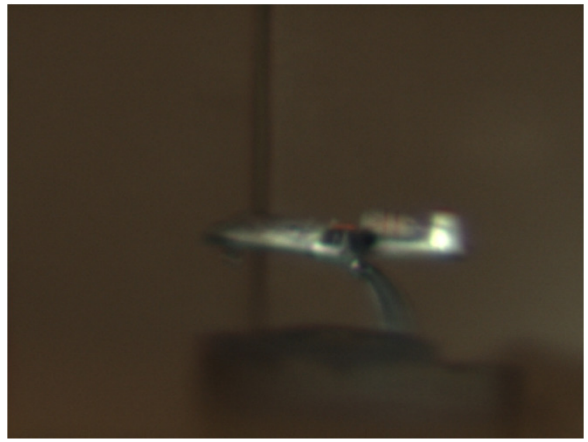

Turbulence in middle of path

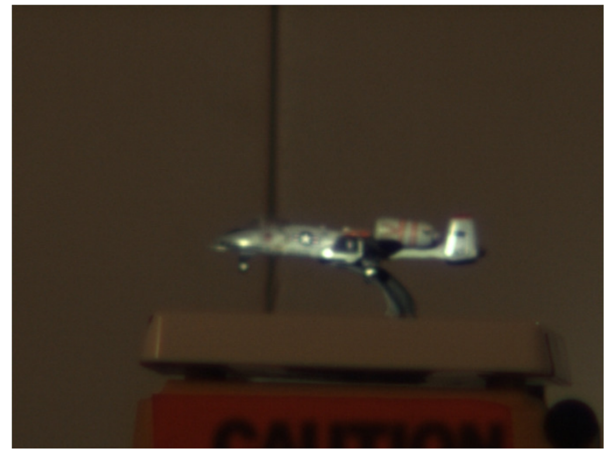

Turbulence near Target

Images of an A10 Warthog taken through local turbulence

Principle of Plenoptic Image Correction

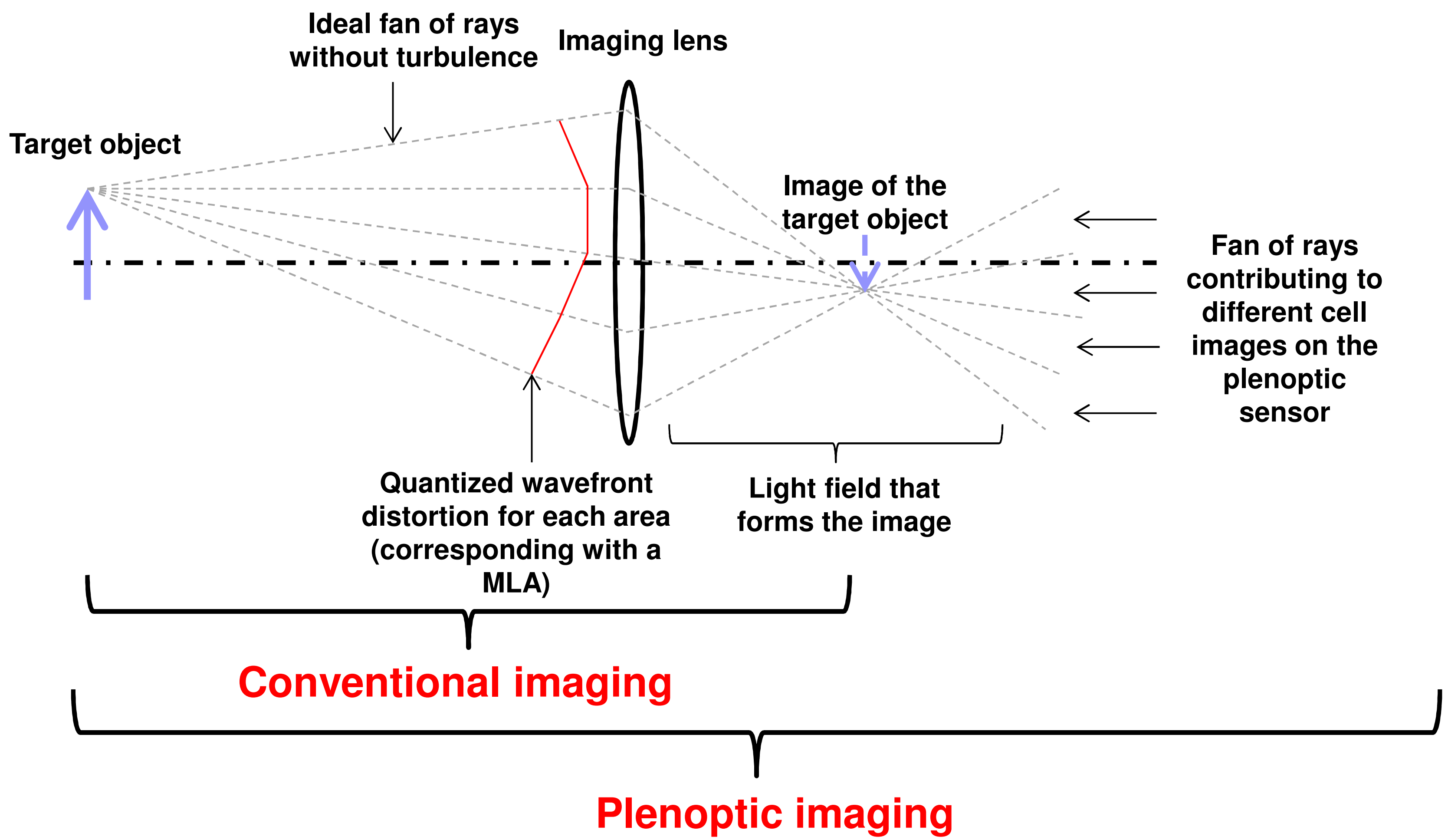

Recall: Structure of a Plenoptic Sensor

Note: the hardware design of the plenoptic sensor features a Keplerian telescope array with shared objective lens.

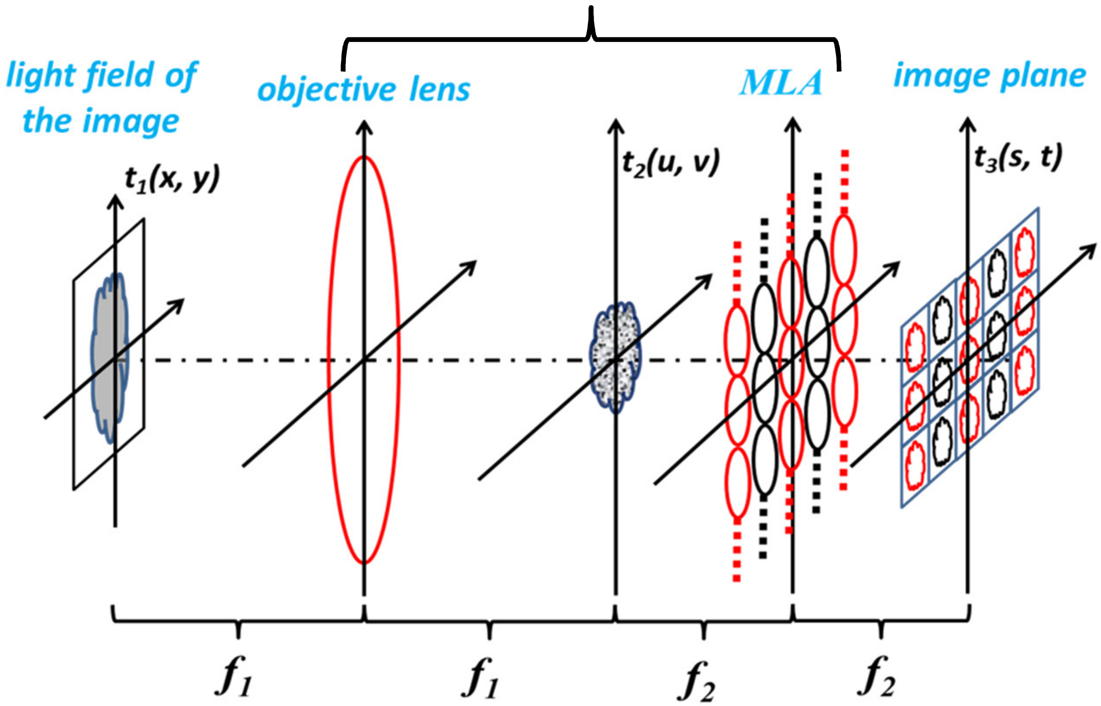

3D Structure Diagram of a Plenoptic Sensor

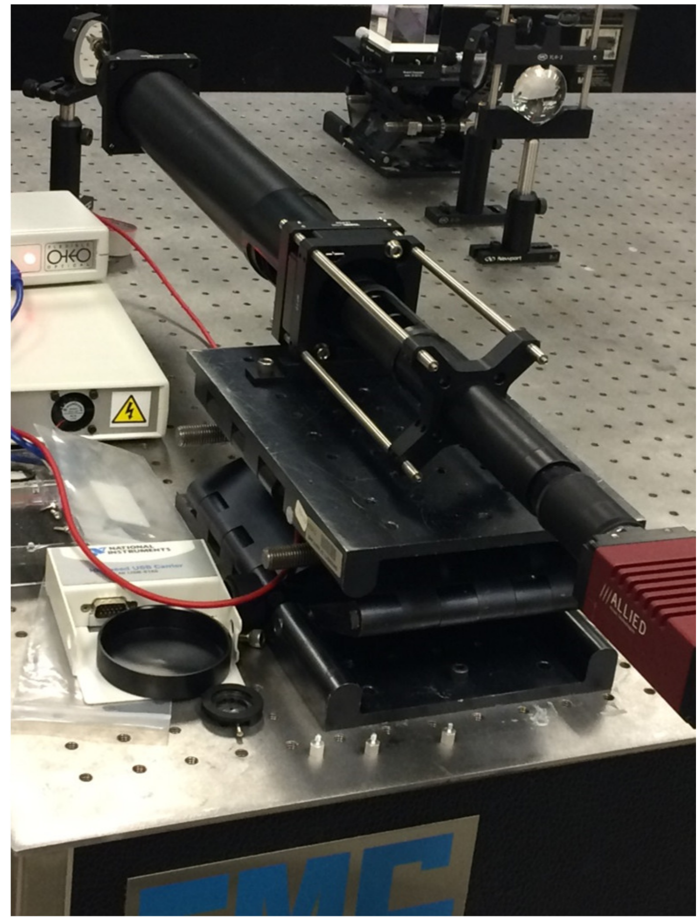

Image of a plenoptic sensor (2nd generation)

Principle of Plenoptic Image Correction

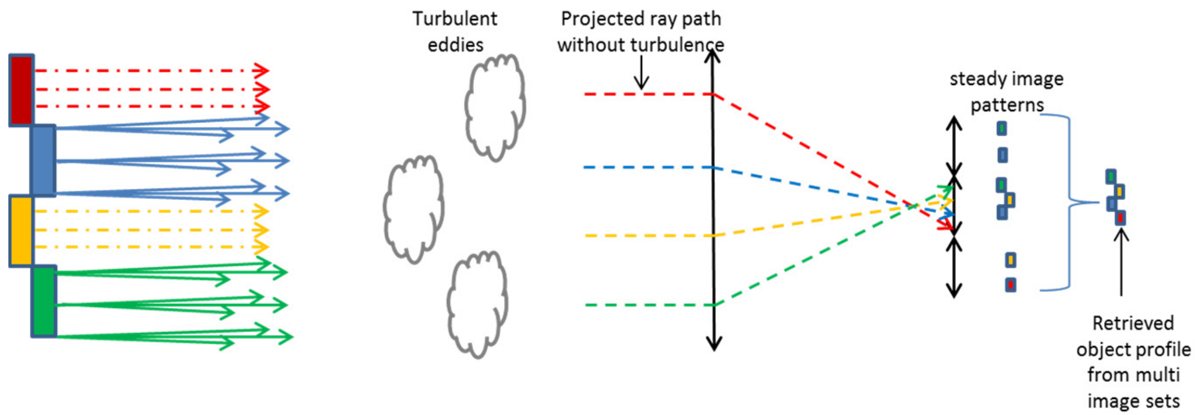

Integration of techniques in hyper dimensional “lucky image”, multi aperture sensing and parallel computing

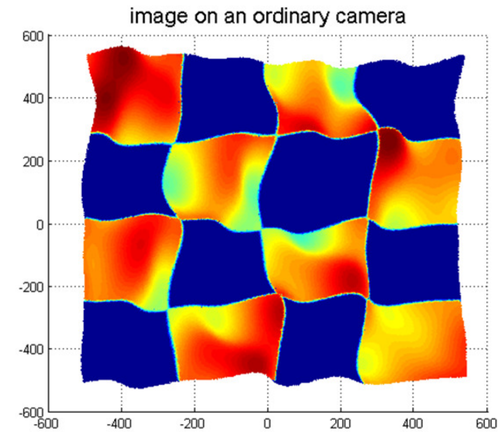

Distorted checkerboard

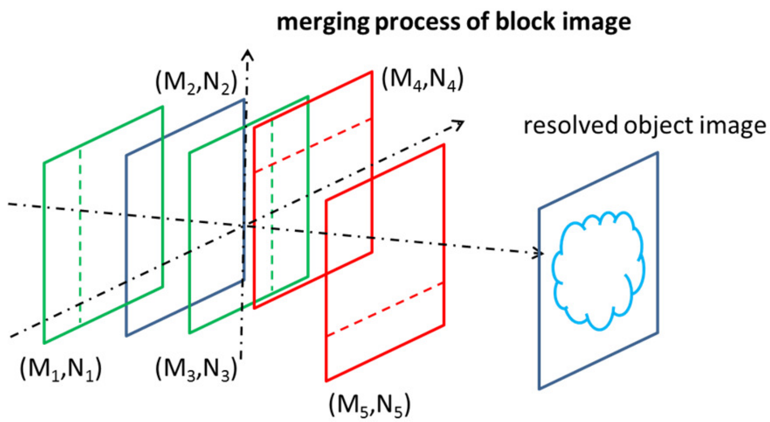

Combine localized images

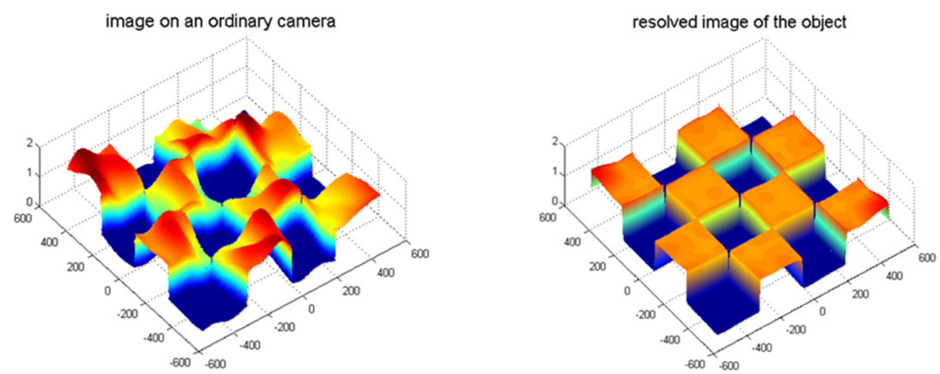

improvements

Principle of Plenoptic Image Correction: a Fast Metric Approach

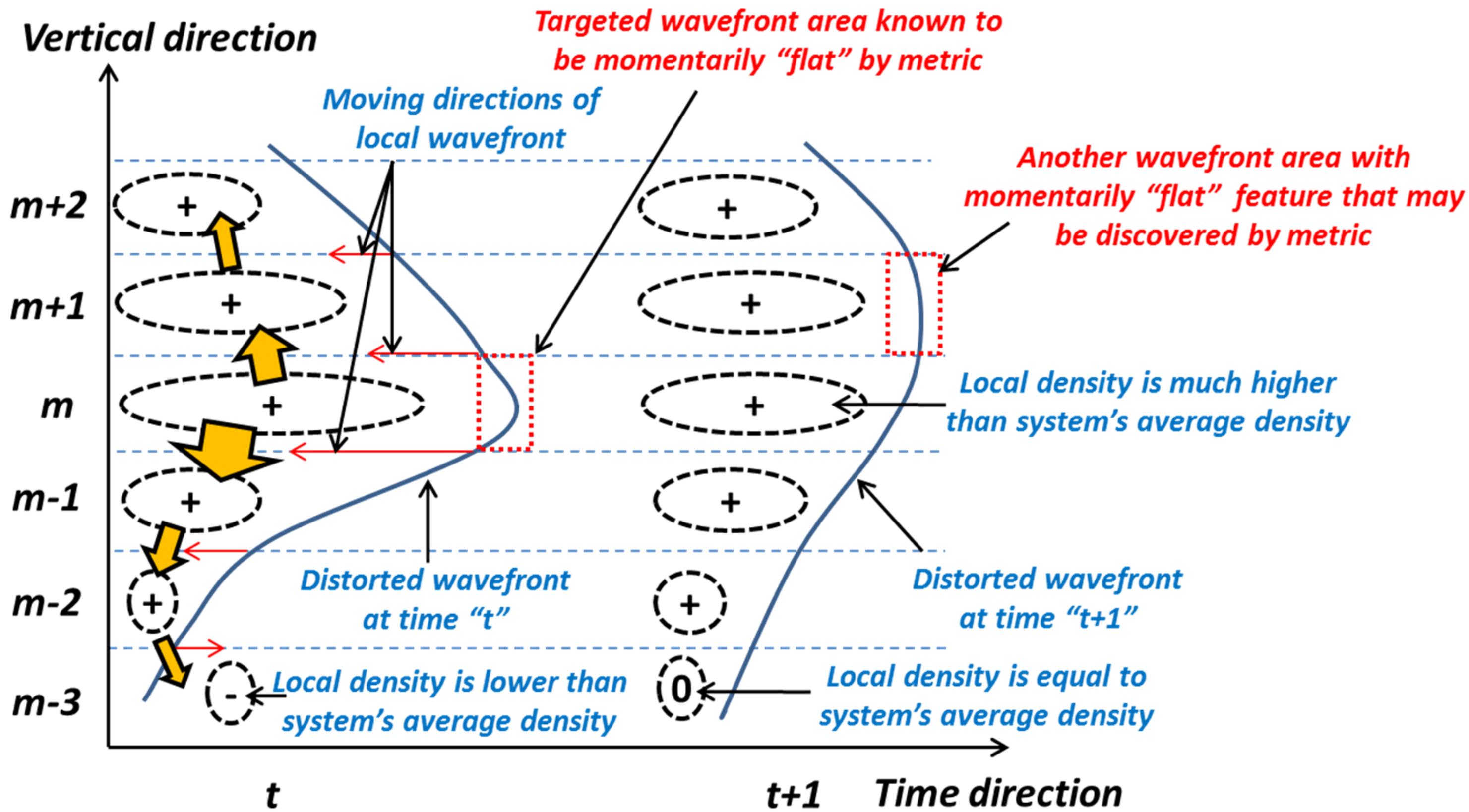

$$M(m,n,t) = a_{vertical}(m,n,t) \cdot a_{horizontal}(m,n,t) \cdot a_{time}(m,n,t)$$

$$a_{time}(m,n,t) = \sqrt{\sum_{i,j} \left[I_{m,n,t+1}(i,j) + I_{m,n,t-1}(i,j) - 2I_{m,n,t}(i,j) \right]^2}$$

Imaging through Turbulent Media

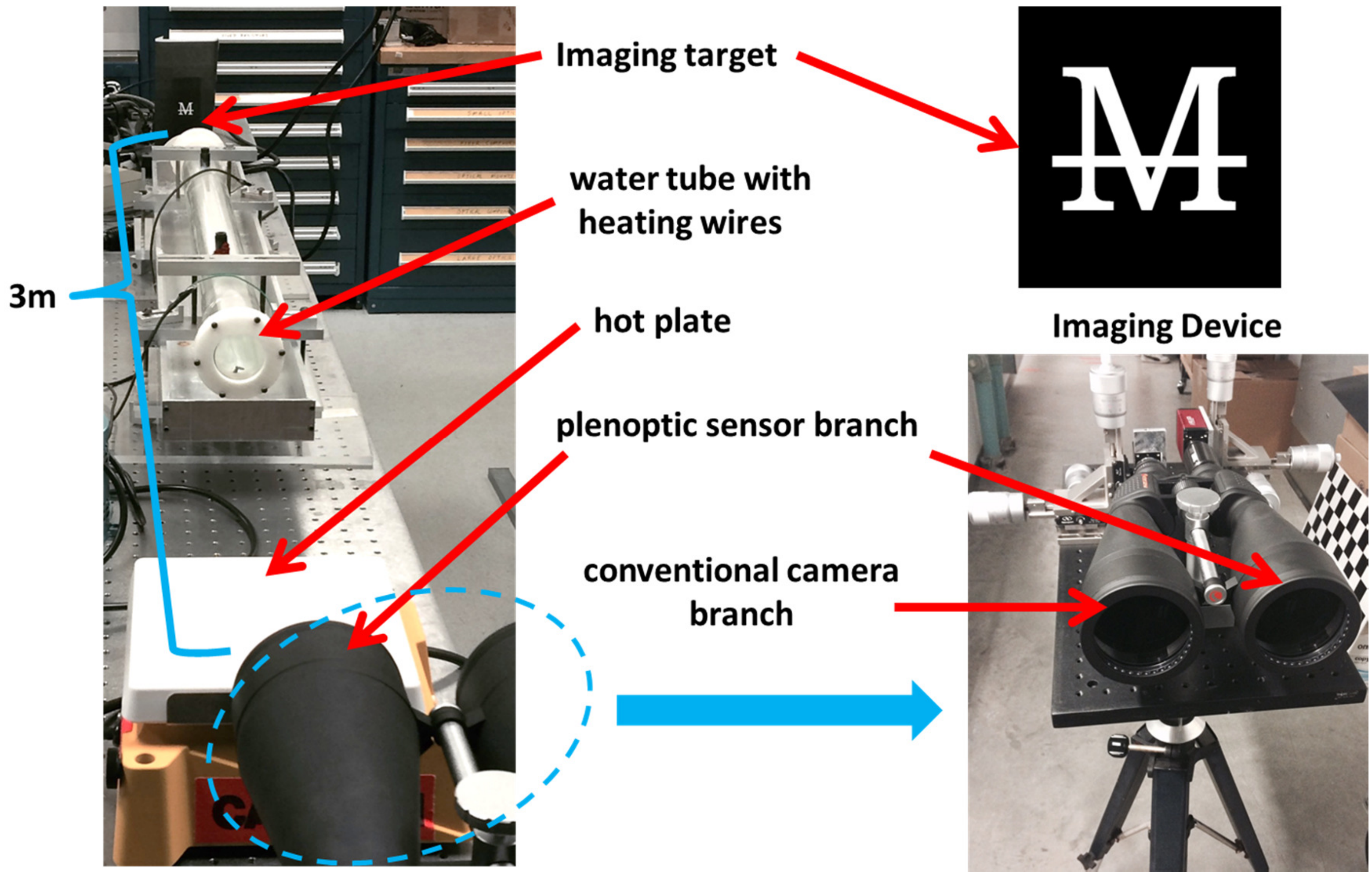

Imaging through Turbulent Media

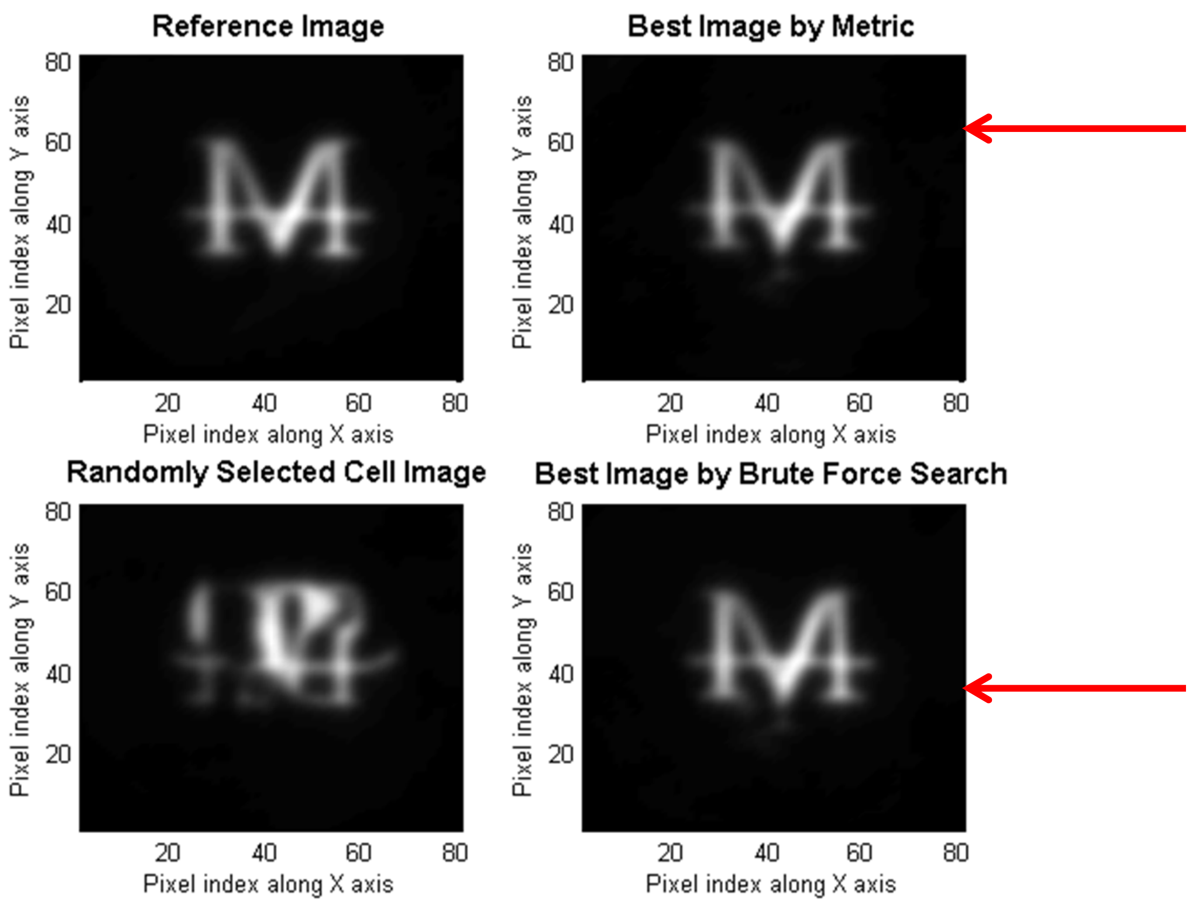

(1) A "mutated" Laplacian metric is used for auto selection.
(2) No external information is used.
(3) 98.09% similar to reference image.

(1) Correlation between each cell image and reference image is exhaustively examined.
(2) The reference image is used.
(3) 98.72% similar to reference image.

Note: **3 types of local wavefront structure can be identified by a large metric value:**

1) valley of a convex; 2) peak of a concave; 3) central area near a saddle point.

Imaging through Turbulent Media

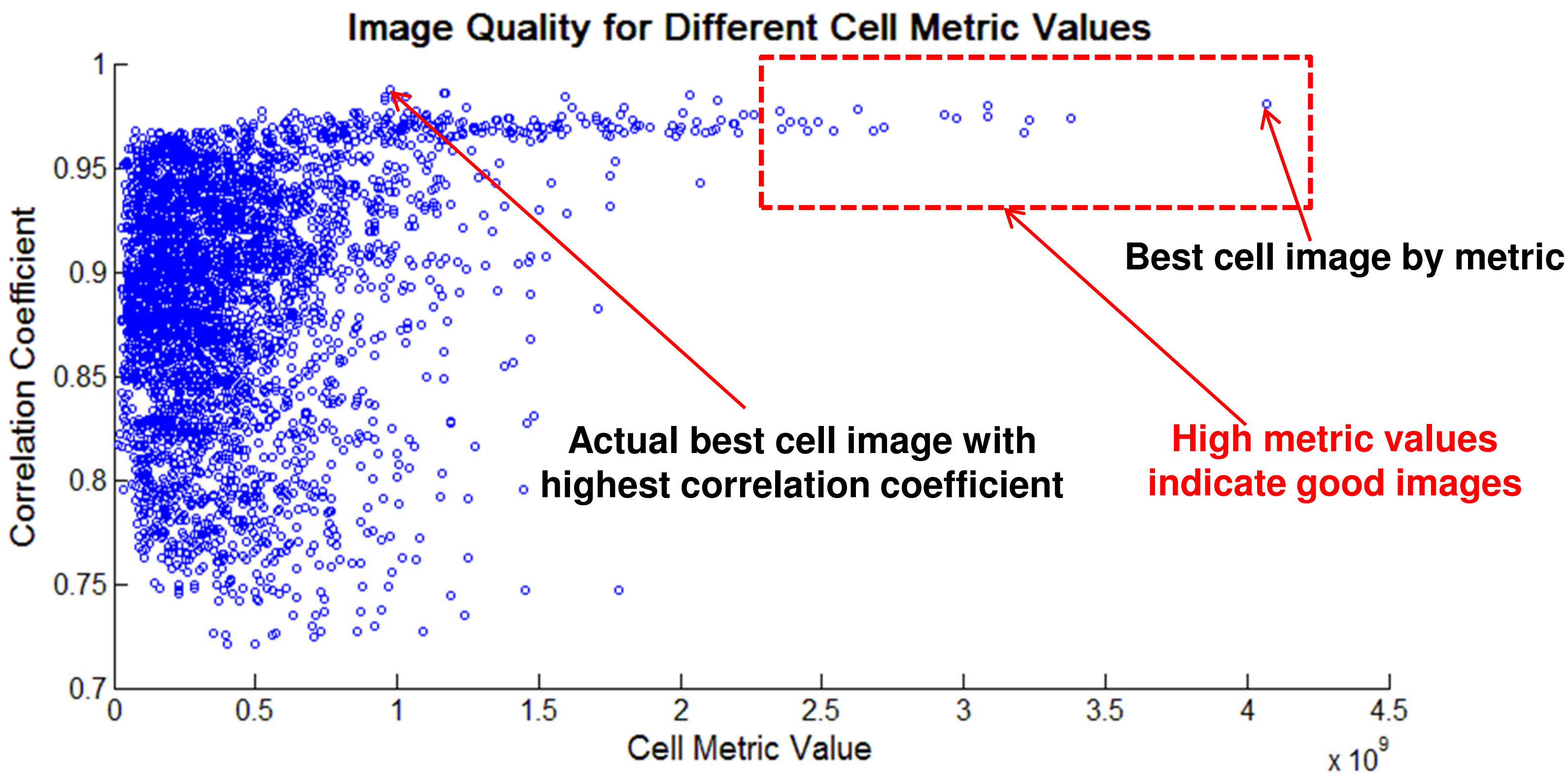

A1: Comprehensive Tool to Study Turbulence Effects on Laser Beams

Plenoptic Sensor at UCF Test Range of 1km

Plenoptic sensor with 6" Cassegrain telescope lens

Lenovo W550S mobile workstation

Power generator

The following data can be acquired simultaneously:

(1) Intensity scintillation.
(2) Angle of arrival scintillation.
(3) C_n^2 estimation over time.
(4) Wavefront shapes over time.

Plenoptic Images of the Distorted Laser Beam (L=960m)

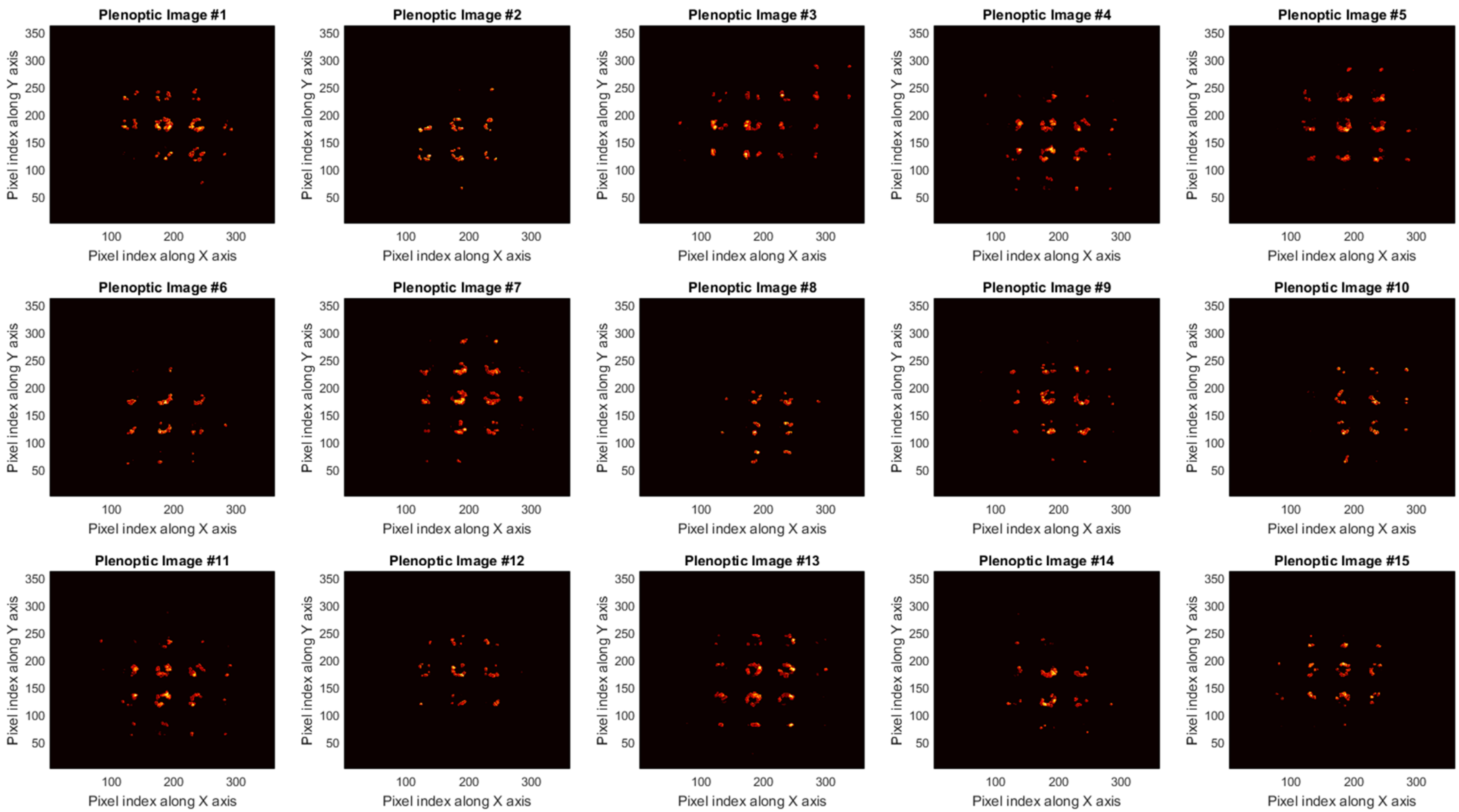

Reconstructed Aperture Intensity Distributions

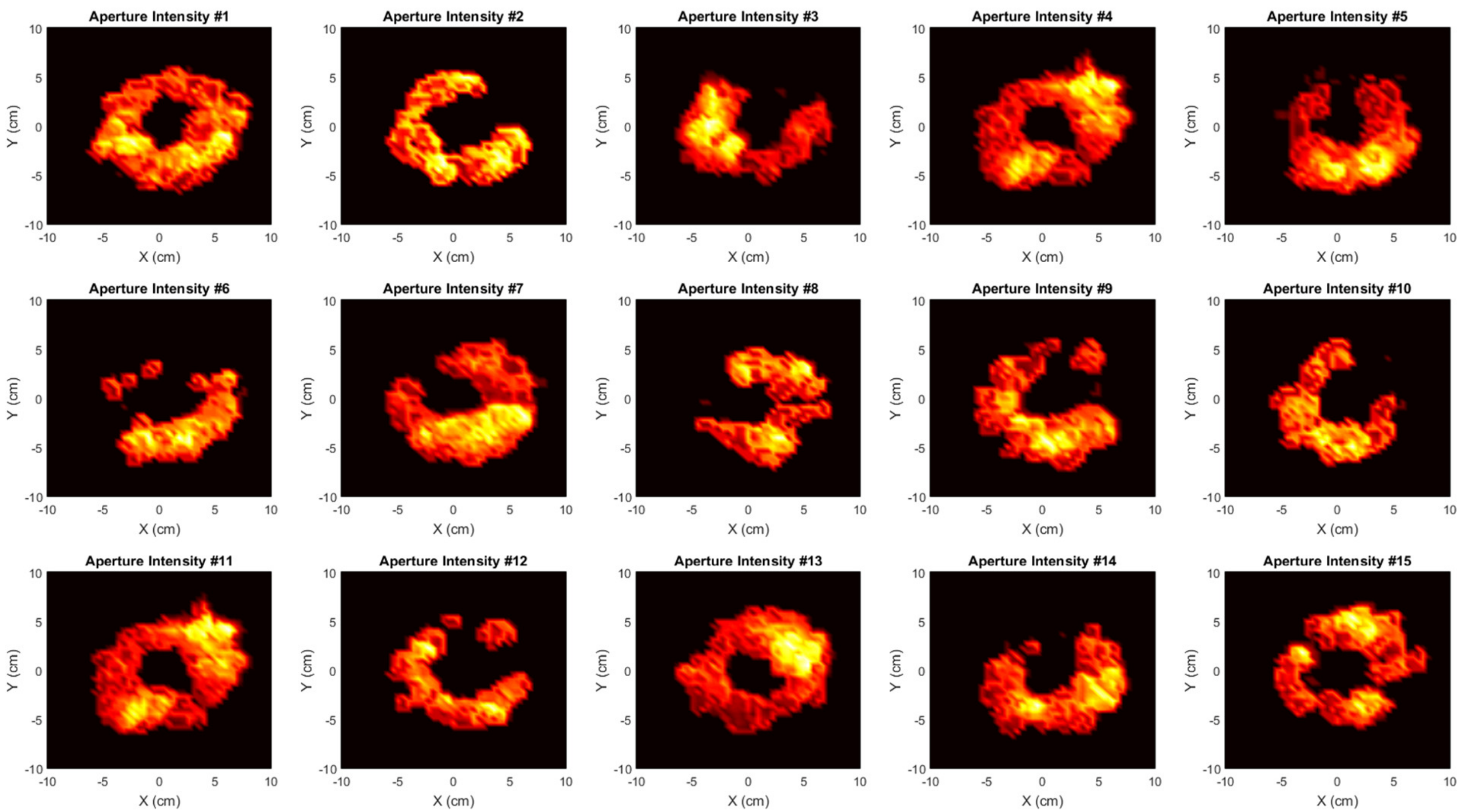

C_n^2 Value Can be Evaluated Based on Intensity Fluctuations

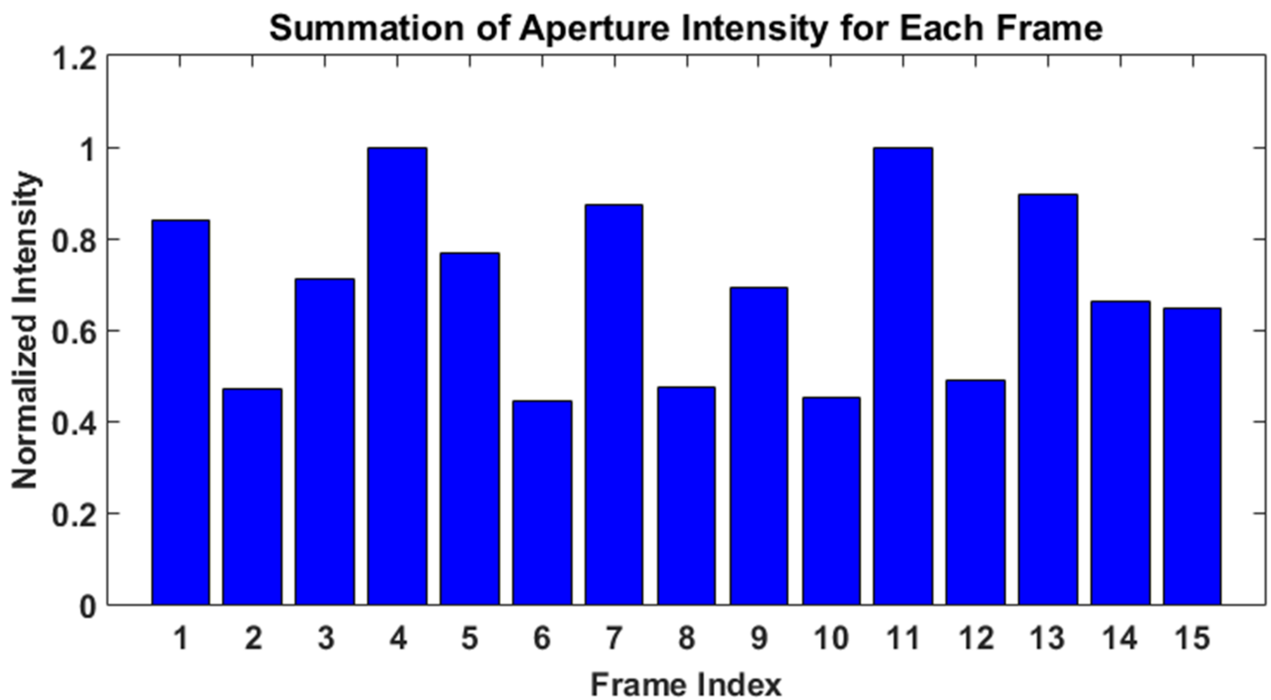

Date & Time: 03/21/2016, 15:09

Calculated result on the plenoptic sensor:

$$C_n^2=7.124\times10^{-13}m^{-2/3}$$

Reference result (by large aperture scintillometer) :

$$C_n^2=8.41\times10^{-13}m^{-2/3}$$

C_n^2 Value Can also be Evaluated Based on Fluctuations in Angle of Arrival

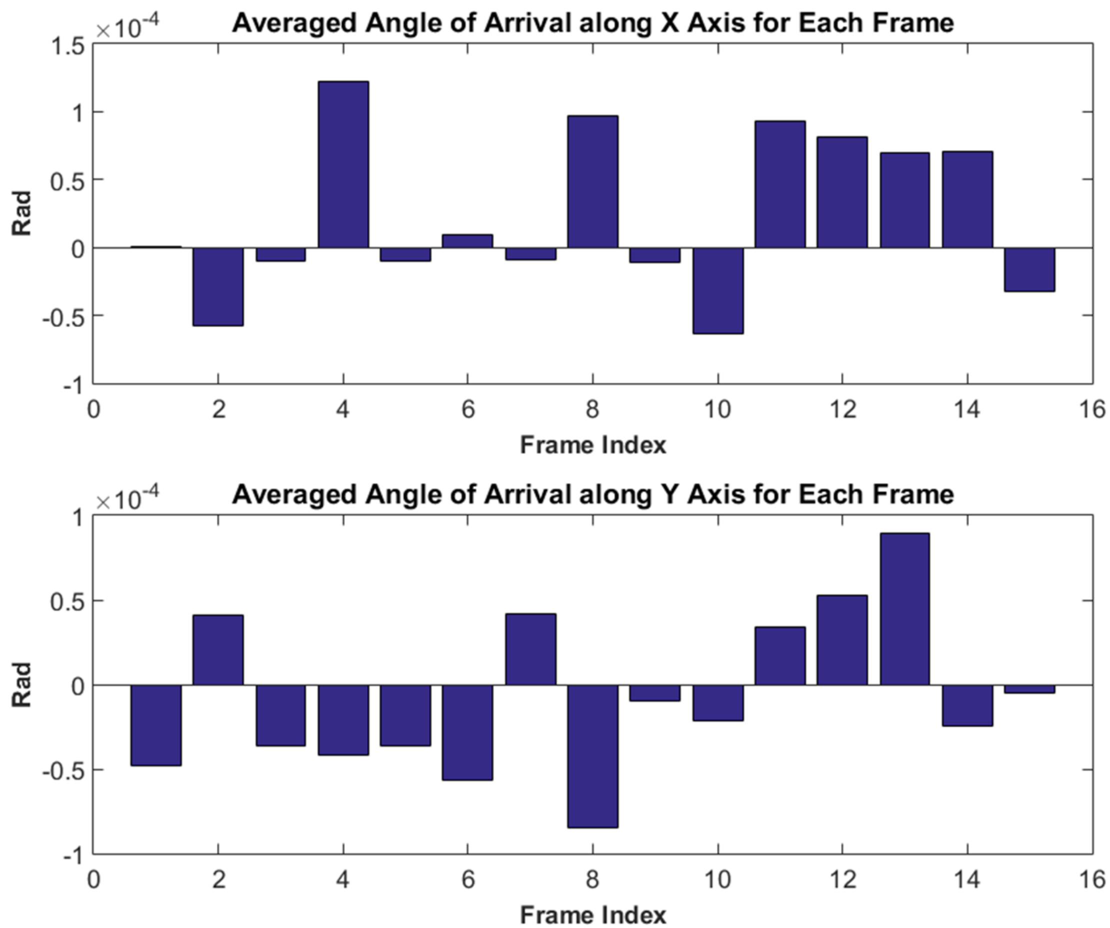

Date & Time: 03/21/2016, 15:09

Estimated C_n^2 contribution by angle of arrival along X axis:

$C_n^2=5.29\times10^{-13}m^{-2/3}$

Estimated C_n^2 contribution by angle of arrival along Y axis:

$C_n^2=6.99\times10^{-13}m^{-2/3}$

Note:

Reference result on previous slide (by the plenoptic sensor):

$C_n^2=7.124\times10^{-13}m^{-2/3}$

Reference result (by large aperture scintillometer) :

$C_n^2=8.41\times10^{-13}m^{-2/3}$

Reconstructed Wavefront Distortion of the Laser Beam

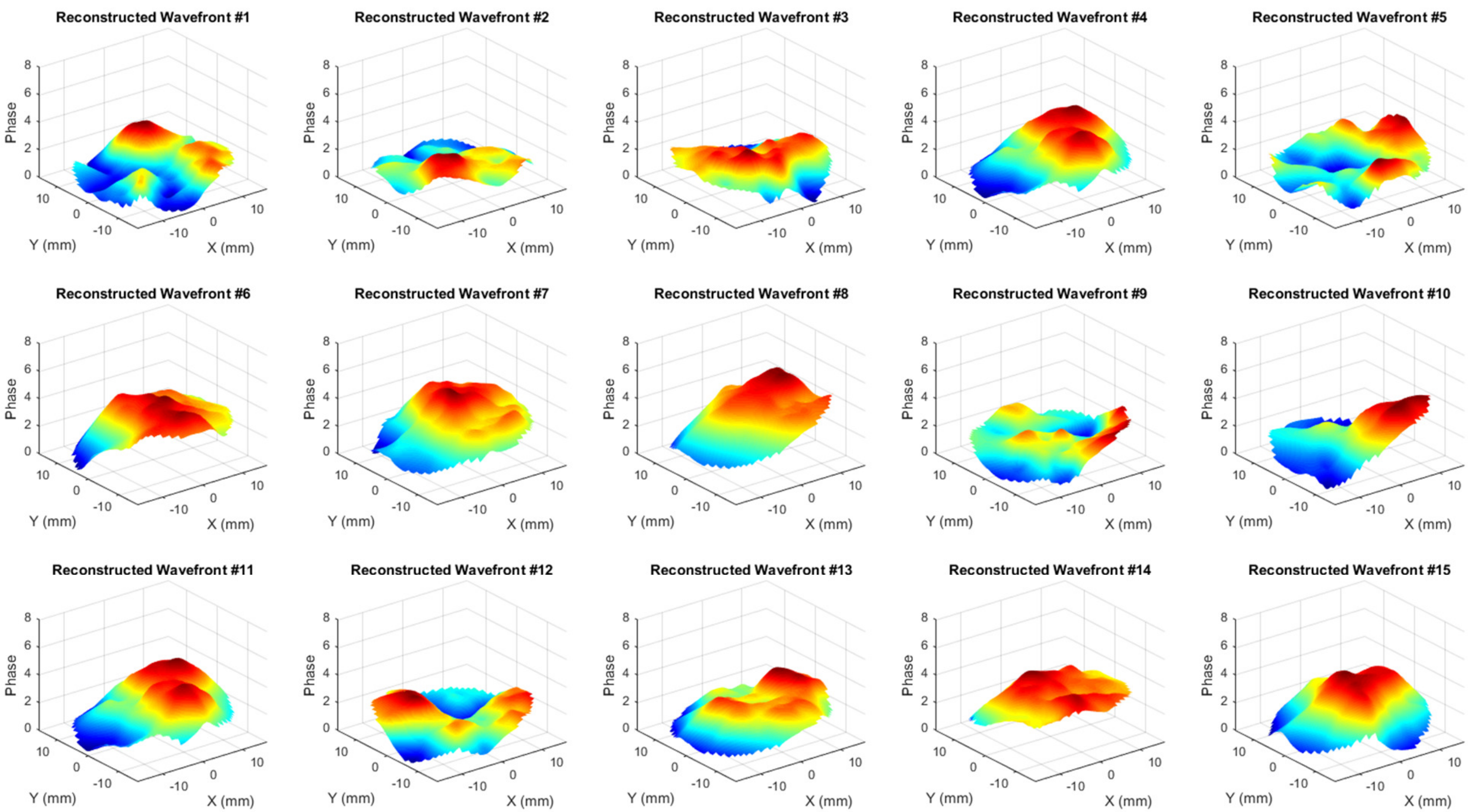

A2: Detecting Vortex Beams (M=4 cell)

M=4 vortex phase cell

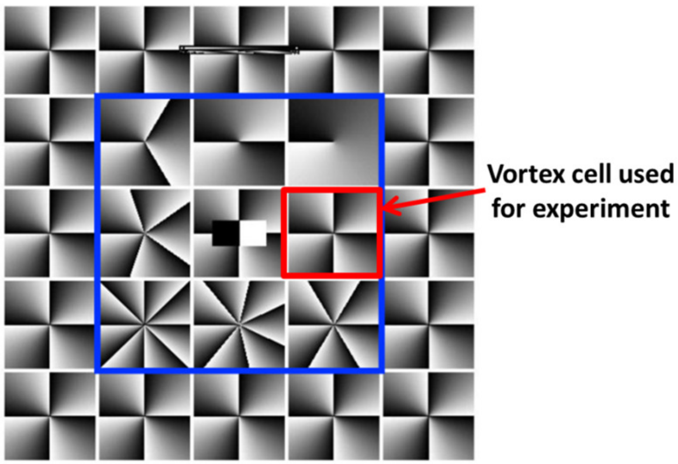

Plenoptic Image of the Vortex Beam

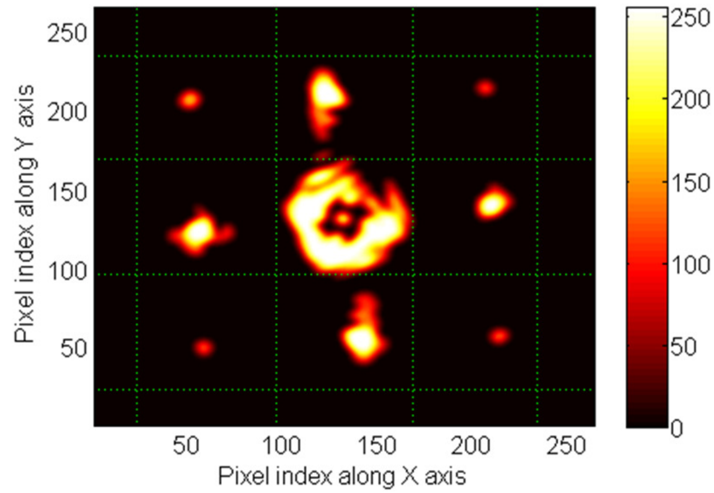

Reconstructed phase gradients

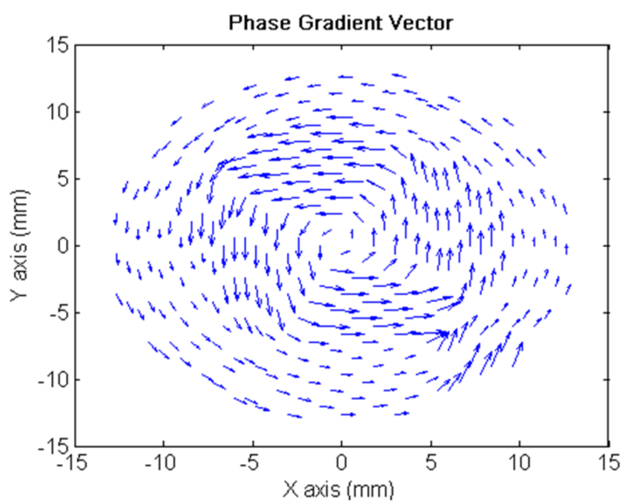

Curl of the phase gradients

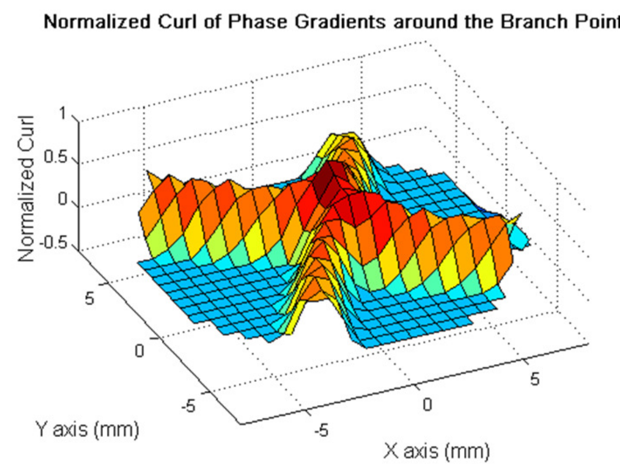

A2: Detecting Vortex Beams (M=4 cell)

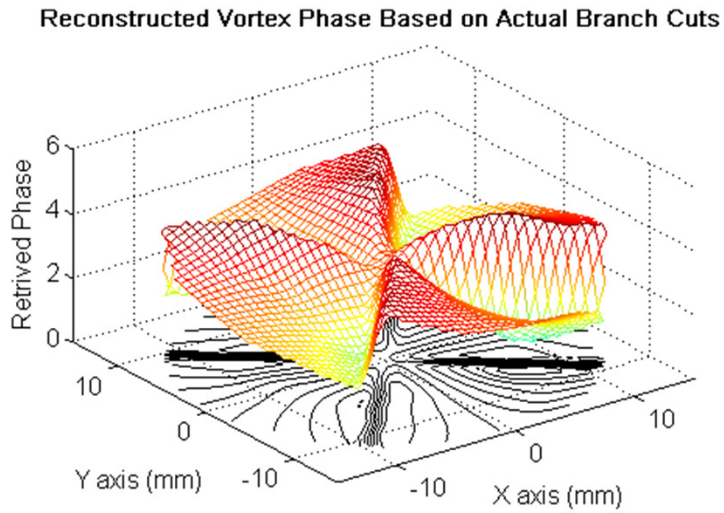

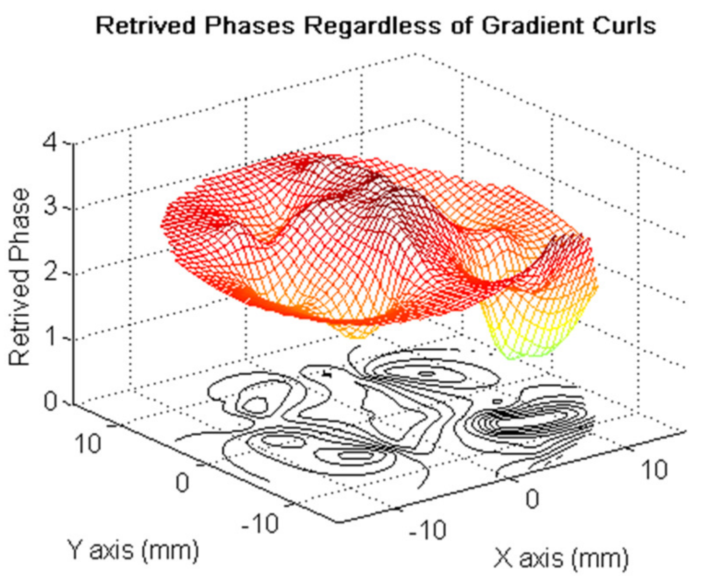

Importance of branch point detection:

(1) Reconstruction will be accurate by considering the non-zero curl of the retrieved phase gradient.

(2) Reconstruction will be incorrect by ignoring the non-zero curl of the retrieved phase gradient.

A2: Detecting Vortex Beams (M=6 cell)

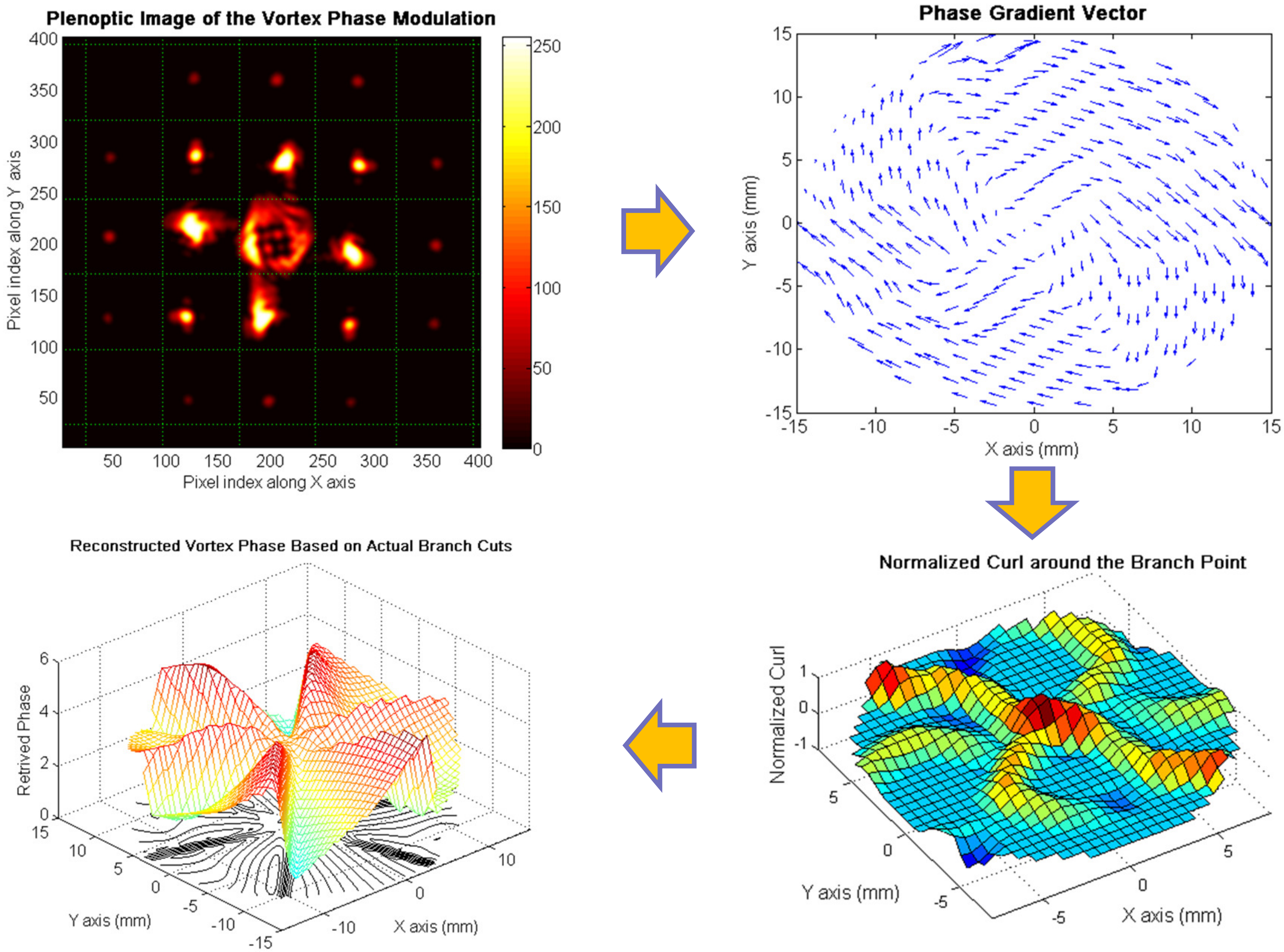

Thank You

List of Publications

2016:

1. **<u>Wu, Chensheng</u>**, Jonathan Ko, and Christopher C. Davis. "Imaging through strong turbulence with a light field approach." *Optics Express* 24.11 (2016): 11975-11986.
2. **<u>Chensheng Wu</u>**, Jonathan Ko, and Christopher C. Davis, "Using a plenoptic sensor to reconstruct vortex phase structures," Opt. Lett. 41, 3169-3172 (2016)
3. W. Nelson, J. P. Palastro, **<u>C. Wu</u>**, and C. C. Davis, "Using an incoherent target return to adaptively focus through atmospheric turbulence," Opt. Lett. 41, 1301-1304 (2016)

2015:

1. **<u>Wu, Chensheng</u>**, Jonathan Ko, and Christopher Davis. "Determining the phase and amplitude distortion of a wavefront using a plenoptic sensor". JOSA A (accepted).
2. **<u>Wu, Chensheng</u>**, Jonathan Ko, and Christopher Davis. "Object recognition through turbulence with a modified plenoptic camera." In *SPIE LASE*, pp. 93540V-93540V. International Society for Optics and Photonics, 2015.
3. **<u>Wu, Chensheng</u>**, Jonathan Ko, and Christopher C. Davis. "Imaging through turbulence using a plenoptic sensor." In *SPIE Optical Engineering+ Applications*, pp. 961405-961405. International Society for Optics and Photonics, 2015.
4. **<u>Wu, Chensheng</u>**, Jonathan Ko, and Christopher C. Davis. "Entropy studies on beam distortion by atmospheric turbulence." In *SPIE Optical Engineering+ Applications*, pp. 96140F-96140F. International Society for Optics and Photonics, 2015.
5. Nelson, W., **<u>C. Wu</u>**, and C. C. Davis. "Determining beam properties at an inaccessible plane using the reciprocity of atmospheric turbulence." In *SPIE Optical Engineering+ Applications*, pp. 96140E-96140E. International Society for Optics and Photonics, 2015.
6. Ko, Jonathan, **<u>Chensheng Wu</u>**, and Christopher C. Davis. "An adaptive optics approach for laser beam correction in turbulence utilizing a modified plenoptic camera." In *SPIE Optical Engineering+ Applications*, pp. 96140I-96140I. International Society for Optics and Photonics, 2015.
7. Nelson, W., J. P. Palastro, **<u>C. Wu</u>**, and C. C. Davis. "Enhanced backscatter of optical beams reflected in turbulent air." *JOSA A* 32, no. 7 (2015): 1371-1378.

List of Publications

2014:

1. **Wu, Chensheng**, William Nelson, and Christopher C. Davis. "3D geometric modeling and simulation of laser propagation through turbulence with plenoptic functions." In *SPIE Optical Engineering+ Applications*, pp. 92240O-92240O. International Society for Optics and Photonics, 2014.
2. **Wu, Chensheng**, William Nelson, Jonathan Ko, and Christopher C. Davis. "Experimental results on the enhanced backscatter phenomenon and its dynamics." In *SPIE Optical Engineering+ Applications*, pp. 922412-922412. International Society for Optics and Photonics, 2014.
3. **Wu, Chensheng**, Jonathan Ko, William Nelson, and Christopher C. Davis. "Phase and amplitude wave front sensing and reconstruction with a modified plenoptic camera." In *SPIE Optical Engineering+ Applications*, pp. 92240G-92240G. International Society for Optics and Photonics, 2014.
4. Nelson, W., J. P. Palastro, **C. Wu**, and C. C. Davis. "Enhanced backscatter of optical beams reflected in atmospheric turbulence." In *SPIE Optical Engineering+ Applications*, pp. 922411-922411. International Society for Optics and Photonics, 2014.
5. Ko Jonathan, **Chensheng Wu**, and Christopher C. Davis. "Intelligent correction of laser beam propagation through turbulent media using adaptive optics." In*SPIE Optical Engineering+ Applications*, pp. 92240E-92240E. International Society for Optics and Photonics, 2014.

2013:

1. **Wu, Chensheng**, and Christopher C. Davis. "Modified plenoptic camera for phase and amplitude wavefront sensing." In *SPIE Optical Engineering+ Applications*, pp. 88740I-88740I. International Society for Optics and Photonics, 2013.
2. **Wu, Chensheng**, and Christopher C. Davis. "Geometrical optics analysis of atmospheric turbulence." In *SPIE Optical Engineering+ Applications*, pp. 88740V-88740V. International Society for Optics and Photonics, 2013.

2012:

1. Eslami Mohammed, **Chensheng Wu**, John Rzasa, and Christopher C. Davis. "Using a plenoptic camera to measure distortions in wavefronts affected by atmospheric turbulence." In *SPIE Optical Engineering+ Applications*, pp. 85170S-85170S. International Society for Optics and Photonics, 2012.